Biodiversity and Climate Change Project - BIOCLIME

Survey of biomass, carbon stocks, biodiversity, and assessment of the historic fire regime for integration into a forest monitoring system in South Sumatra, Indonesia.

Project number: 12.9013.9-001.00

Survey of biomass, carbon stocks, biodiversity, and assessment of the historic fire regime for integration into a forest monitoring system in the Districts Musi Rawas, Musi Rawas Utara, Musi Banyuasin and Banyuasin, South Sumatra, Indonesia

Overarching Report Work Packages 1-4

Final Report

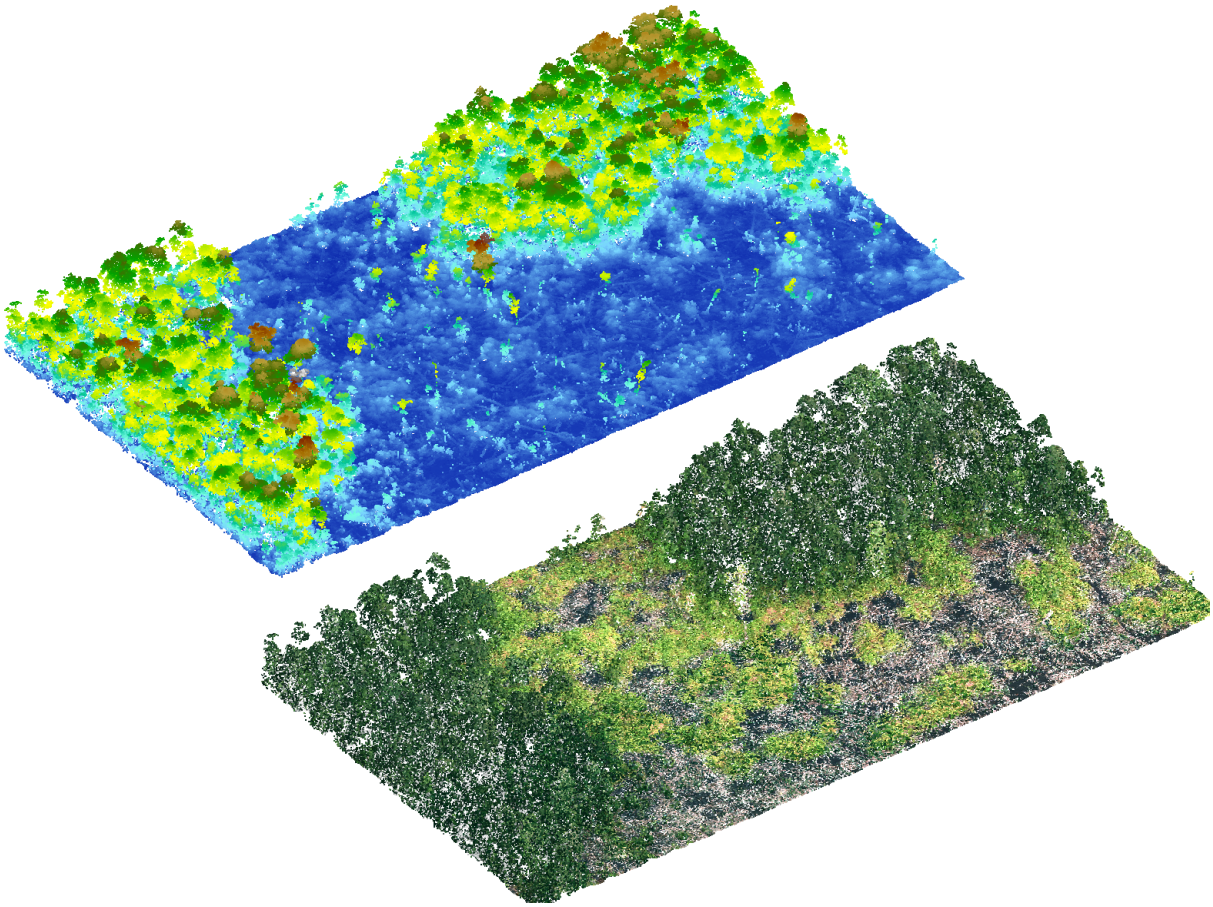

Prepared by:

Dr. Uwe Ballhorn, Peter Navratil, Dr. Sandra Lohberger, Matthias Stängel, Werner Wiedemann, Kristina Konecny, Prof Dr. Florian Siegert

RSS – Remote Sensing Solutions GmbH

Isarstraße 3

82065 Baierbrunn

Germany

Phone: +49 89 48 95 47 66

Fax: +49 89 48 95 47 67

Email: ballhorn@rssgmbh.de

November 2016

Table of Content

1. Introduction

With the Biodiversity and Climate Change Project (BIOCLIME), Germany supports Indonesia's efforts to reduce greenhouse gas emissions from the forestry sector, to conserve forest biodiversity of High Value Forest Ecosystems, maintain their Carbon stock storage capacities and to implement sustainable forest management for the benefit of the people. Germany's immediate contribution will focus on supporting the Province of South Sumatra to develop and implement a conservation and management concept to lower emissions from its forests, contributing to the GHG emission reduction goal Indonesia has committed itself until 2020.

One of the important steps to improve land-use planning, forest management and protection of nature is to base the planning and management of natural resources on accurate, reliable and consistent geographic information. In order to generate and analyze this information, a multi-purpose monitoring system is required.

This system will provide a variety of information layers of different temporal and geographic scales:

- Information on actual land-use and the dynamics of land-use changes during the past decades is considered a key component of such a system. For South Sumatra, this data is already available from a previous assessment by the World Agroforestry Center (ICRAF).
- Accurate current information on forest types and forest status, in particular in terms of aboveground biomass, carbon stock and biodiversity, derived from a combination of remote sensing and field techniques.
- Accurate information of the historic fire regime in the study area. Fire is considered one of the key drivers shaping the landscape and influencing land cover change, biodiversity and carbon stocks. This information must be derived from historic satellite imagery.
- Indicators for biodiversity in different forest ecosystems and degradation stages.

The objective of the work conducted by Remote Sensing Solutions GmbH (RSS) was to support the goals of the BIOCLIME project by providing the required information on land use dynamics, forest types and status, biomass and biodiversity and the historic fire regime. The conducted work is based on a wide variety of remote sensing systems and analysis techniques, which were jointly implemented within the project, in order to produce a reliable information base able to fulfil the project's and the partners' requirements on the multi-purpose monitoring system.

This report summarizes the main objectives, methodological approaches, results and conclusions from Work Packages 1 – 4:

- Work Package 1 (WP 1): Historic land cover change and carbon emission baseline
- Work Package 2 (WP 2): Forest benchmark mapping and monitoring
- Work Package 3 (WP 3): Aboveground biomass and tree community composition modelling
- Work Package 4 (WP 4): Historic fire regime

Figure 1 gives an overview of the location four BIOCLIME districts and nine project areas within South Sumatra (Indonesia).

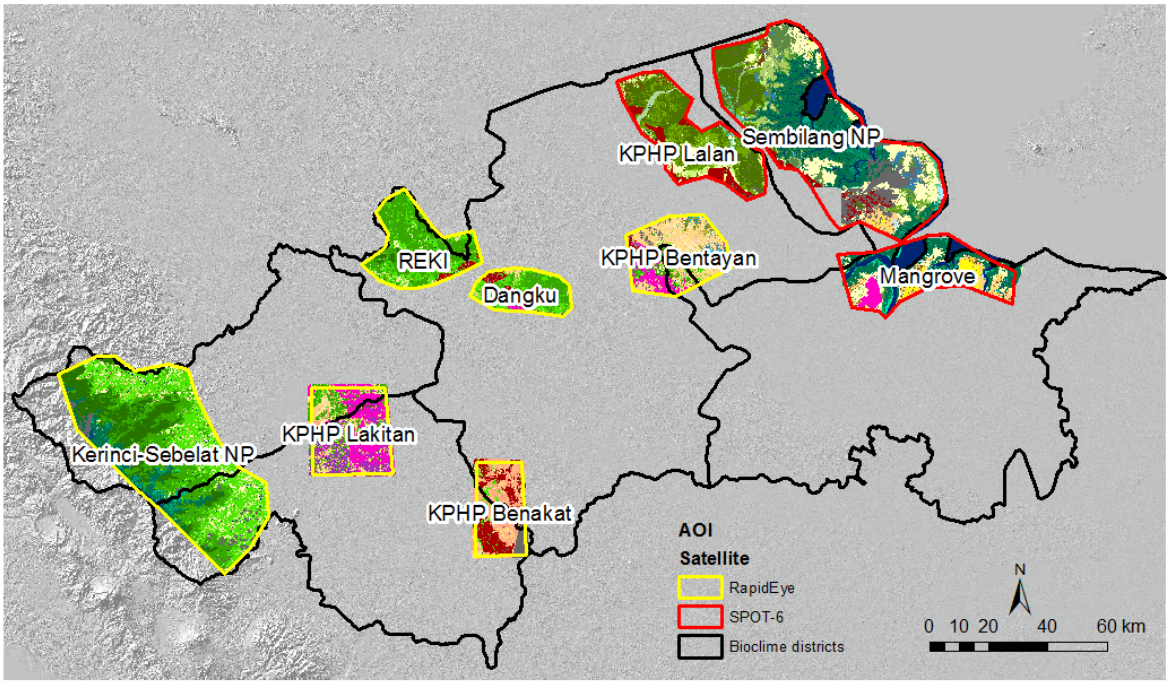

Figure 1: The BIOCLIME districts and the nine project areas.

2. Concept of the monitoring system

The four Work Packages mentioned above form the basis of the developed monitoring system. The concept of the monitoring system consists of three components: historical, current and monitoring (Figure 2). The historical component includes an analysis of the historic fire regime on the basis of Landsat imagery (WP 4: Historic fire regime) as well as historic land cover change maps produced by ICRAF (international Center for Research in Agroforestry) in order to identify drivers of deforestation and carbon emissions (WP 1: Historic land cover change and carbon emission baseline). The current component comprises the development the development of aboveground biomass and tree community composition models from airborne LiDAR data (WP 3: Aboveground biomass and tree community composition modelling) as well as a forest benchmark map derived from high resolution satellite images (WP 2: Forest benchmark mapping and monitoring) in order to create and retrieve local aboveground biomass values (WP 3: Aboveground biomass and tree community composition modelling). The main objectives, methodological approaches, results and conclusions for each of the Work Packages is described in the following text. A more detailed description of these Work Packages is given the respective Work Package final reports.

As the derived local aboveground biomass values build up the basis for the carbon stock and emission calculations in WP 1, WP 2 and WP 4 it was decided to first describe Work Package 3 (Aboveground biomass modelling and tree community composition modelling).

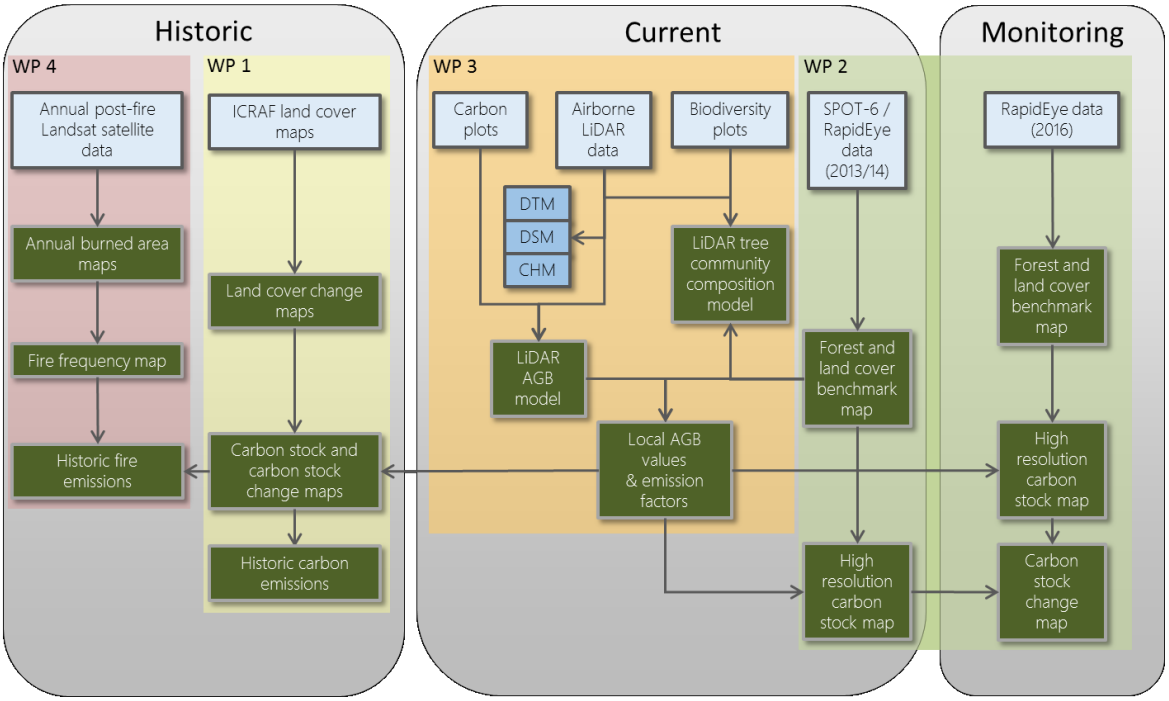

Figure 2: Concept of the monitoring system. Also shown is which parts of the monitoring system are covered by which Work Packages: WP 1 (Work Package 1): Historic land cover change and carbon emission baseline; WP 2 (Work Package 2): Forest benchmark mapping and monitoring; WP 3 (Work Package 3: Aboveground biomass and tree community composition modelling; WP 4 (Work Package 4): Historic fire regime.

3. Objectives

3.1. Work Package 3 (WP 3): Aboveground biomass and tree community composition

- Filtering of the LiDAR 3D point clouds (provided by the project) into vegetation and non-vegetation points.
- Derive Digital Surface Models (DSM), Digital Terrain Models (DTM) and Canopy Height Models (CHM) from the airborne LiDAR data.
- Advice BIOCLIME in the collection of forest inventory data to calibrate the LiDAR derived aboveground biomass model.
- Derive an aboveground biomass model from the airborne LiDAR data (provided by the project) in combination with forest inventory data (provided by the project).
- Deduce local aboveground biomass values for different vegetation classes from this LiDAR based aboveground biomass model.
- Derive a tree a community composition model of Lowland Dipterocarp Forest at various degradation stages from LiDAR data (provided by the project) in combination with tree species/genera diversity data collected in the field (provided by the project).

3.2. Work Package 1 (WP 1): Historic land cover change and carbon emission baseline

- Assessment of the historic land cover (1990, 2000, 2005, 2010 and 2014) in the four BIOCLIME districts based on a historic land cover data set (Version 3) provided by the World Agroforestry Center (ICRFA).
- Derivation and assessment of the historic land cover change and dynamics based on this dataset.
- Derivation and assessment of the historic carbon stocks based on this data set and local aboveground biomass values derived in Work Package 3 (WP 3): Aboveground biomass and tree community composition modelling.
- Derivation and assessment of the carbon stock changes derived from these carbon stock estimates in order to contribute to the calculation of the reference emission level (REL).
- Derivation of an emission baseline in order to contribute to the calculation of the reference emission level (REL).

3.3. Work Package 2 (WP 2): Forest benchmark mapping and monitoring were:

- Preprocessing of high resolution satellite images (SPOT and RapidEye) for the project areas KPHP Benakat, KPHP Bentayan, Dangku Wildlife Reserve, Kerinci Seblat National Park, KPHP Lakitan, KPHP Lalan, Mangrove, PT Reki and Sembilang National Park for the years 2014 and 2016.
- Derivation and assessment of the land cover for 2014 (forest benchmark) and 2016 (monitoring) based on these high resolution satellite images.
- Derivation and assessment of the land cover change and dynamics between 2014 and 2016.
- Derivation and assessment of the carbon stocks based on the above derived land cover and the local aboveground biomass values from Work Package 3 (WP 3): Aboveground biomass and tree community composition modelling.
- Derivation and assessment of the carbon stock changes derived from these carbon stock estimates.

3.4. Work Package 4 (WP 4): Historic fire regime were:

- Selection of annual mid resolution satellite images (Landsat) for the fire years 1990-2014 covering the four BIOCLIME districts.
- Preprocessing of these mid resolution satellite images (Landsat).
- Derivation and assessment burned areas for these fire years based on these mid resolution satellite images (Landsat).
- Derivation and assessment of the aboveground biomass fire emissions based on these yearly classified burned areas, the historical land covers derived in Work Package 1 (WP 1): Historic land cover change and carbon emission baseline and the local aboveground biomass values from Work Package 3 (WP 3): Aboveground biomass and tree community composition modelling.

- Derivation and assessment of the peat fire emissions based on these yearly classified burned areas, a peatland distribution map provided by the Ministry of Environment and Forestry (MoEF), the historical land covers derived in Work Package 1 (WP 1): Historic land cover change and carbon emission baseline and peat burned depths based on a publication by Konecny *et al.* (2015).

4. Methodological approaches and results

4.1. Work Package 3 (WP 3): Aboveground biomass and tree community composition

Figure 3 shows the flowchart of the activities carried out in Work Package 3 (WP 3): Aboveground biomass and tree community composition modelling.

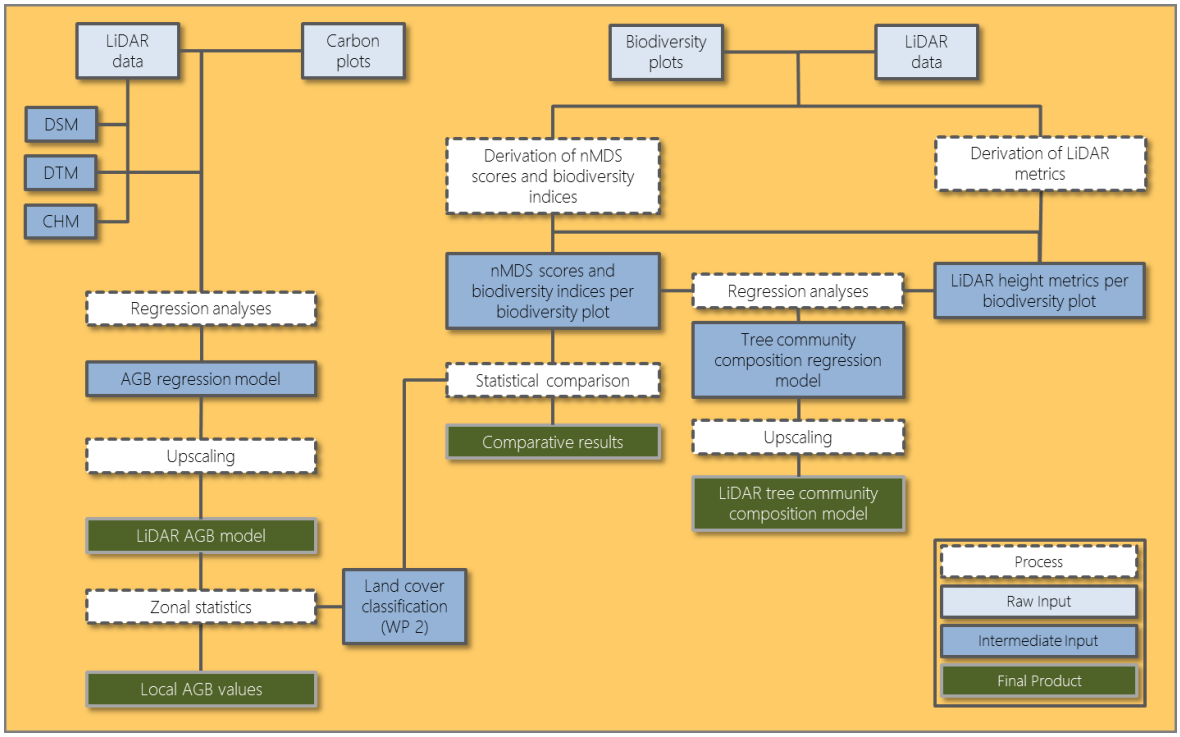

Figure 3: Flow chart of the activities carried out in Work Package 3 (WP 3): Aboveground biomass and tree community composition modelling.

4.1.1. Carbon and biodiversity plots

115 plots forest inventory plots were recorded within the four districts of Banyuasin, Musi Banyasin, Musi Rawas Utara and Musi Rawas. All these districts are located in the province of South Sumatra. The planning and collection of these so called carbon inventory plots was conducted by scientists of the Bogor Agricultural University (IPB) and BIOCLIME. The distribution of these carbon inventory plots is based on a systematic sampling design. In order, to assure that statistically enough carbon inventory plots are located within the airborne LiDAR transects to generate the LiDAR based aboveground biomass model some of these 115 plots where spatially shifted into the nearest LiDAR transect, consequently now not fitting into the systematic sampling design anymore. In natural forests a nested rectangular plot design was chosen (0.1 ha) and in plantations a circular plot design was applied, where the size of the

circle depended on the age of the plantation (age of plantation < four years: radius = 7.98 m, area = 0.02 ha; age of plantation ≥ four years: radius = 11.29 m, area = 0.04 ha). For all "in" trees (an "in" tree was defined as a tree where the center of the stem at DBH was within the boundaries of the respective (sub)plot) Diameter at Breast Height (DBH; in centimeter), total tree height (in meter), trees species (scientific name in Latin) and four dead wood classes were recorded.

Additionally, to the carbon plots 59 so called biodiversity plots were recorded. The spatial locations of these biodiversity plots are exactly the same as the ones of the respective carbon plot. For all "in" trees within the biodiversity plots Diameter at Breast Height (DBH; in centimeter) and tree species (scientific name in Latin) were recorded.

Table 1 gives an overview on how many carbon and biodiversity plots were recorded and whether they are located within LiDAR transects or not. As can be seen in Table *1*, six plots were recorded after the fires of 2015. These plots have to be treated with care, as the LiDAR data was recorded before the fires of 2015.

Table 1: Overview carbon and biodiversity plots recorded and whether they are located within LiDAR transects or not.

Carbon plots	Biodiversity plots	Amount plots	Amount plots within LiDAR transects
X		56 (54[1])	17 (15[1])
X	X	59 (55[1])	49 (45[1])
	Sum	**115 (109[1])**	**66 (60[1])**

[1] Amount of plots after subtracting plots that were recorded after the fires of 2015

Figure 4 displays the location of the recorded carbon and biodiversity plots within the four districts of Banyuasin, Musi Banyasin, Musi Rawas Utara and Musi Rawas. It also shows which of these carbon and biodiversity plots are located within a LiDAR transect.

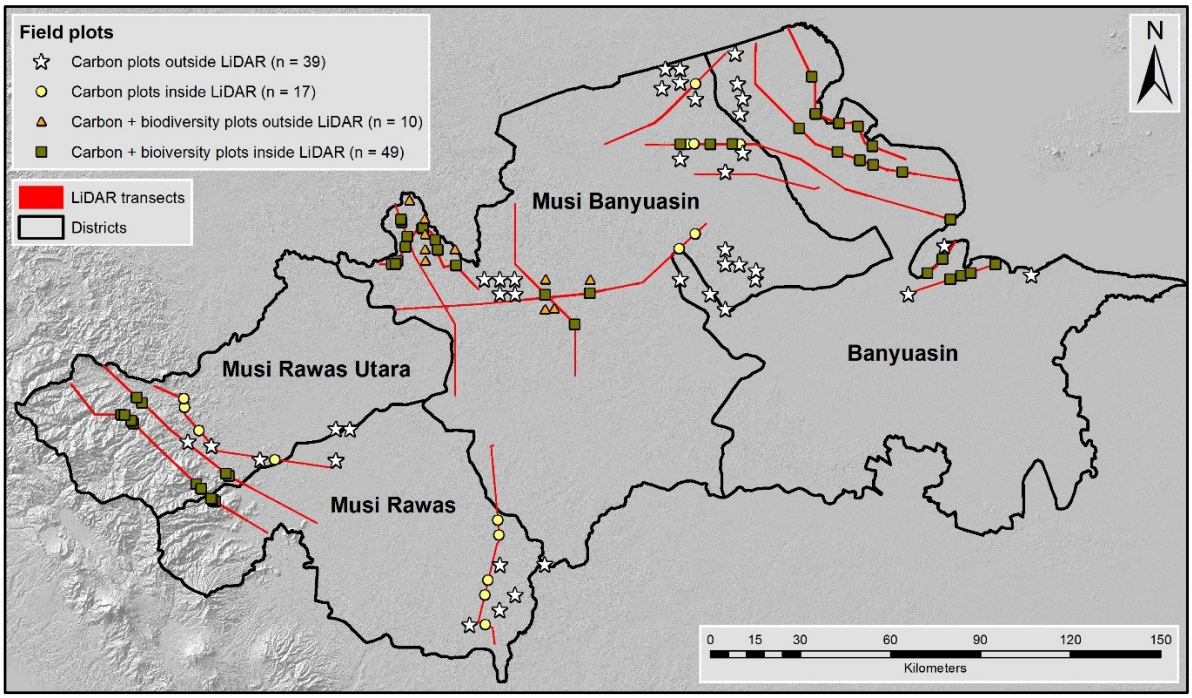

Figure 4: Location of all recorded carbon and biodiversity plots within the four districts of Banyuasin, Musi Banyasin, Musi Rawas Utara and Musi Rawas. Also shown is which of these carbon and biodiversity plots are located within a LiDAR transect.

4.1.2. Aboveground biomass calculations

First the species-specific wood densities for the recorded trees were derived based on the Latin scientific names and an established wood density database (Zanne *et al.* 2009). If a tree could not be identified or only identified to the genus or family level or the common name an average wood density of 0.57 g/cm^3 for South East Asia (tropical) trees from this data base was attributed. Table 2 displays the absolute numbers and percentage of trees within the carbon plots where the species could be identified, where only genus, family, common name was known and unidentified trees.

Table 2: Absolute and percentage of tree identification (species, only genus, only family, only common name and unidentified) within the carbon plots.

	All trees recorded	Species identified	Only genus identified	Only family identified	Only common name	Unidentified
Absolute number	2038	1105	272	18	605	38
Percent (%)	100%	54%	13%	1%	30%	2%

Next, for trees where absolute tree height was not measured a tree height model was derived based on DBH (1,851 tree height measurements were used as input to the model development).

Finally, to estimate aboveground biomass per tree (palm) three different allometric equations, depending on the tree (palm) type, were applied. Table 3 displays the allometric equations used for the different tree (palm) types.

Table 3: Allometric equations used to estimate above ground biomass depending on the tree (palm) type.

	Mangrove trees	Oil palms	All other trees
Allometric equation	Moist mangrove forest stands $AGB_{est}=\exp(-2.977+\ln(pD^2H))$	$AGB_{est}=71.797*H-7.0872$	Best fit pantropical model $AGB_{est}=0.0673*(pD^2H)^{0.976}$
Source	Chave *et al.* 2005	Asari *et al.* 2013	Chave *et al.* 2014

AGB_{est} = estimated aboveground biomass, p = wood specific density (in g/cm³), D = diameter at breast height (in cm) and H = total tree (palm) height (in m)

The aboveground biomass estimates per tree were summed up per plot and then expanded to one hectare to get aboveground biomass estimates per hectare. Aboveground biomass estimates for the biodiversity plots were calculated the same way.

4.1.3. LiDAR data and aerial photos

In October 2014 15 transects of LiDAR data and aerial photos were captured for an area of approximately 43,300 ha. LiDAR data was acquired in two modes (a) LiDAR full waveform mode + aerial photos with an overlap of 60% and (b) LiDAR discrete return mode + aerial photo overlap 80%. Figure 4 shows the location of the LiDAR transects within the BIOCLIME study area.

Different types of elevation models were generated from the airborne LiDAR 3D point clouds. Figure 5 shows some LiDAR 3D point could example sections representing different forest types (Lowland Dipterocarp Forest, Peat Swamp Forest and Mangrove).

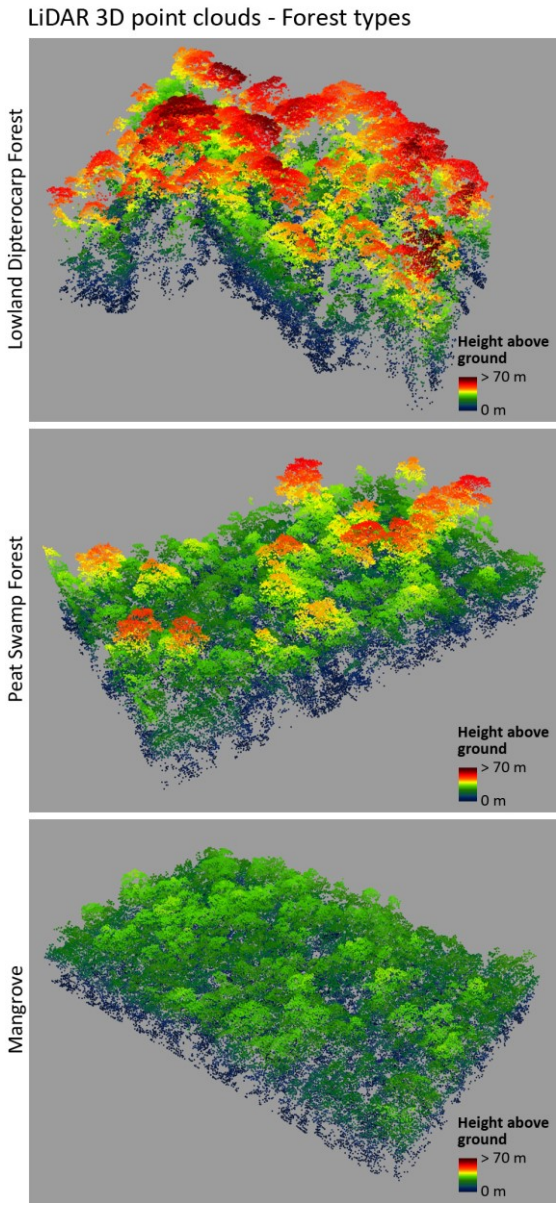

Figure 5: Example of LiDAR 3D point clouds for Lowland Dipterocarp Forest, Peat Swamp Forest and Mangrove.

Products derived from these LiDAR 3D point clouds include a Digital Surface Model (DSM) which represents the elevation of the vegetation canopy, a Digital Terrain Model (DTM) which represents the ground elevation, and a Canopy Height Model (CHM) which is generated by subtraction of the DTM from the DSM and represents the vegetation height. The LiDAR data was processed using the Trimble Inpho software package. Figure 6 exemplarily shows the resulting models for the BIOCLIME study area. Also shown are the positions of the field plots (n = 66) which are located within the LiDAR transects.

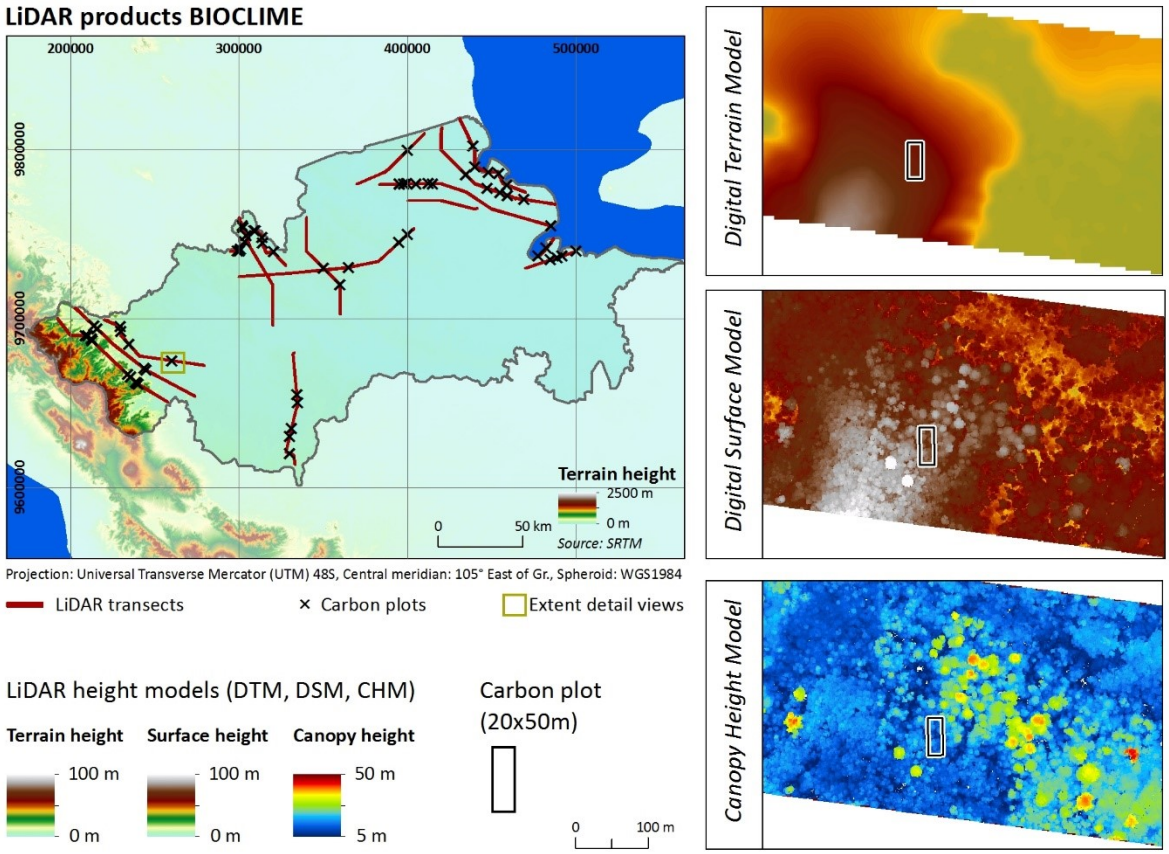

Figure 6: Example from the LiDAR products generated for the BIOCLIME study area. Shown are examples for the Digital Terrain Model (DTM; 1 m spatial resolution) the Digital Surface Model (DSM; 1 m spatial resolution) and the Canopy Height Model (CHM; 1 m spatial resolution). Also shown are the position of the 66 carbon plots that are located within the LiDAR transects.

4.1.4. LiDAR based aboveground biomass model

Previous studies revealed that height metrics like the Quadratic Mean Canopy Height (QMCH) or the Centroid Height (CH) are appropriate parameters of the LiDAR 3D point cloud to estimate aboveground biomass in tropical forests (Jubanski *et al.* 2013, Englhart *et al.* 2013, Ballhorn *et al.* 2011). QMCH and CH calculated at carbon plot location and correlated to field inventory estimated of aboveground biomass and regression models were developed. Jubanski *et al.* (2013) showed that the accuracy of the aboveground biomass estimations derived from LiDAR height histograms increased with higher point densities. For this reason, point density was also implemented in the regression as a weighting factor.

Of the 66 carbon plots that were located within the LiDAR transects 54 plots (after removal of obvious outliers) were used for calibration. The model based on QMCH (r^2 = 0.70; n = 54) achieved better results as the one based on CH. Next a spatially explicit aboveground biomass model was created by applying the above described regression model. The LiDAR based aboveground biomass model was created at 5 m spatial resolution i.e. each pixel represents an area of 0.1 ha. For ease of interpretation the cell values

were scaled to represent aboveground biomass in tons per hectare. Figure 7 displays the final LiDAR based aboveground biomass model and gives examples of Lowland Dipterocarp Forest, Peat Swamp Forest and Mangrove.

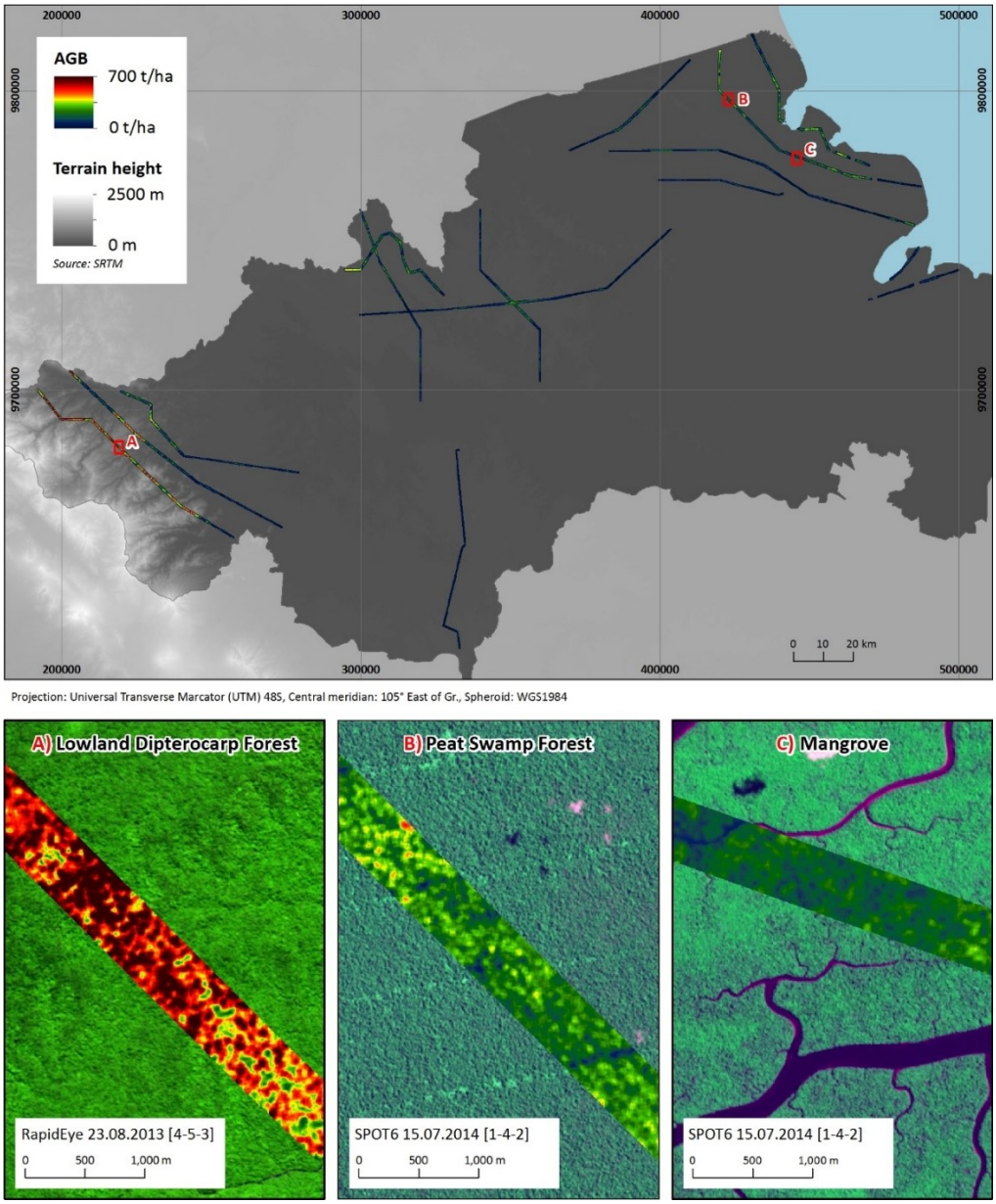

Figure 7: Final LiDAR based aboveground biomass model and examples of Lowland Dipterocarp Forest, Peat Swamp Forest and Mangrove (lower three figures). The location of the lover three figures is shown as red rectangles in the upper figure.

4.1.5. Determination of local aboveground biomass values

In order to derive local aboveground biomass values for the different land cover classes, the spatial aboveground biomass model was overlaid with the land cover classification from Work Package 2 (WP 2) and zonal statistics (minimum, maximum, mean and standard deviation) on aboveground biomass were extracted for the respective land cover class.

Zonal statistics were extracted for the BAPLAN and BAPLAN enhanced land cover classes. Table 4 and Table 5 display these derived local aboveground biomass values. For the land cover classes not present in the aboveground biomass model missing values were estimated based on existing values or missing values were based on values from scientific literature.

These local aboveground biomass values were used for the emission calculations in the other work packages (WP 1, WP 2 and WP 4).

Table 4: Local aboveground biomass values derived from zonal statistics of the LiDAR aboveground biomass model for the different forest type / land cover classes based on BAPLAN.

Forest type / land cover BAPLAN[1]	Mean AGB (t/ha)[2]	SD (t/ha)[3]	Min AGB (t/ha)[4]	Max AGB (t/ha)[5]	Area (ha)[6]
Primary Dryland Forest	545	±165.5	20.8	1,405.0	2,285.2
Secondary / Logged over Dryland Forest	256	±160.3	0.0	1.196.8	5,685.3
Primary Swamp Forest	226	±97.2	1.8	674.3	1,806.5
Secondary / Logged over Swamp Forest	74	±64.4	0.0	460.5	1,363.3
Primary Mangrove Forest	198	±102.7	0.0	632.2	4,031.9
Secondary / Logged over Mangrove Forest	44	±25.1	6.4	228.5	71.7
Mixed Dryland Agriculture / Mixed Garden	105	±84.1	0.0	677.8	1,883.0
Tree Crop Plantation	32	±47.2	0.0	380.2	442.2
Plantation Forest	40	±32.2	0.0	356.7	517.5
Scrub	25	±42.6	0.0	730.4	964.6
Swamp Scrub	8	±11.8	0.0	81.6	3.3
Rice Field[7]	10	-	-	-	-
Dryland Agriculture	31	±47.9	0.0	441.2	126.3
Grass[8]	6	-	-	-	-
Open Land[9]	(0) 20	±65.9	0.0	716.4	13.4
Settlement / Developed Land[9]	(0) 12	±8.6	0.1	50.6	1.3
Water Body[9]	(0) 118	±58.5	0.3	422.2	83.2
Swamp	12	±12.3	0.1	49.9	1.3
Embankment[9]	(0) 1	±1.9	0.0	12.8	9.5

[1] Forest type/land cover class BAPLAN classification system
[2] Mean aboveground biomass (AGB) in tons per hectare for the forest type/land cover class
[3] Standard deviation (SD) in tons per hectare for the forest type/land cover class
[4] Minimum aboveground biomass (AGB) in tons per hectare for the forest type/land cover class
[5] Maximum aboveground biomass (AGB) in tons per hectare for the forest type/land cover class
[6] Area in hectare from which zonal statistics are based on
[7] Value for Rice Field from scientific literature (Confalonieri *et al.* 2009)
[8] Value for Grass from scientific literature (IPCC 2006)
[9] Value in brackets was finally used as local aboveground biomass value as the value from zonal statistics is obviously too high due to misclassification

Table 5: Local aboveground biomass values derived from zonal statistics of the LiDAR aboveground biomass model for the different forest type / land cover classes based on BAPLAN enhanced.

Forest type / land cover BAPLAN enhanced[1]	Mean AGB (t/ha)[2]	SD (t/ha)[3]	Min AGB (t/ha)[4]	Max AGB (t/ha)[5]	Area (ha)[6]
High-density Upper Montane Forest[7]	304	-	-	-	-
Medium-density Upper Montane Forest[8]	228	-	-	-	-
Low-density Upper Montane Forest[7]	192	-	-	-	-
High-density Lower Montane Forest	615	±135.5	171.8	1,092.0	52.0
Medium-density Lower Montane Forest	486	±81.2	306.0	758.3	5.5
Low-density Lower Montane Forest[7]	268	-	-	-	-
High-density Lowland Dipterocarp Forest	543	±165.8	20.8	1,405.0	2,233.2
Medium-density Lowland Dipterocarp Forest	289	±157.1	0.0	1,196.8	4,536.6
Low-density Lowland Dipterocarp Forest	122	±84.7	0.1	966.1	1,143.2
High-density Peat Swamp Forest	235	±99.7	2.1	674.3	1,430.7
Medium-density Peat Swamp Forest[8]	176	-	-	-	-
Low-density (Regrowing) Peat Swamp Forest	77	±73.7	0.3	460.5	590.7
Permanently Inundated Peat Swamp Forest	192	±83.9	1.8	526.4	301.1
High-density Swamp Forest (incl. Back- and Freshwater Swamp)	200	±49.4	6.2	348.8	74.8
Medium-density Swamp Forest (incl. Back- and Freshwater Swamp)[8]	150	-	-	-	-
Low-density (Regrowing) Swamp Forest (incl. Back- and Freshwater Swamp)	73	±56.1	0.0	396.5	772.6
Heath Forest[7]	224	-	-	-	-
Mangrove 1	216	±97.7	0.0	632.2	3,473.1
Mangrove 2	153	±86.7	13.4	471.0	86.0
Nipah Palm	77	±29.6	0.3	409.3	472.8
Degraded Mangrove	46	±25.5	6.4	161.5	57.8
Young Mangrove	39	±22.8	8.4	228.5	13.9
Dryland Agriculture mixed with Scrub	23	±33.2	0.0	464.0	414.2
Rubber Agroforestry	129	±79.4	0.0	677.8	1,468.8
Oil palm plantation	16	±29.6	0.0	282.6	304.2
Coconut plantation	35	±18.2	0.9	88.7	94.1
Rubber	135	±57.4	0.2	380.2	43.9
Acacia plantation	41	±33.7	0.0	178.7	360.2
Industrial forest	39	±28.6	0.1	356.7	157.3
Scrubland	25	±42.6	0.0	730.4	964.6
Swamp Scrub	8	±11.8	0.0	81.6	3.3
Rice Field[9]	10	-	-	-	-
Dryland Agriculture	31	±47.9	0.0	441.2	126.3
Grassland[10]	6	-	-	-	-
Bare Area[11]	(0) 20	±65.9	0.0	716.4	13.4
Settlement[11]	(0) 5	±8.7	0.1	50.6	0.4
Road[11]	(0) 15	±6.2	0.1	28.2	0.9
Water[11]	(0) 118	±58.5	0.3	422.6	83.2
Wetland	12	±12.3	0.1	49.9	1.3
Aquaculture[11]	(0) 1	±1.9	0.0	12.8	9.5

[1] Forest type/land cover class BAPLAN enhanced classification system
[2] Mean aboveground biomass (AGB) in tons per hectare for the forest type/land cover class
[3] Standard deviation (SD) in tons per hectare for the forest type/land cover class
[4] Minimum aboveground biomass (AGB) in tons per hectare for the forest type/land cover class
[5] Maximum aboveground biomass (AGB) in tons per hectare for the forest type/land cover class
[6] Area in hectare from which zonal statistics are based on
[7] Values from FORCLIME (Navratil 2012)
[8] Calculated as 75% of respective high density class
[9] Value for Rice Field from scientific literature (Confalonieri *et al.* 2009)
[10] Value for Grass from scientific literature (IPCC 2006)
[11] Value in brackets was finally used as local aboveground biomass value as the value from zonal statistics is obviously too high due to misclassification

4.1.6. LiDAR based tree community composition model

Within all the biodiversity plots 378 types of species where identified belonging to 192 genera. Table 6 displays the absolute numbers and percentage of trees within the biodiversity plots where the species could be identified, where only genus, family, common name was known and unidentified trees.

Table 6: Absolute and percentage of tree identification (species, only genus, only family, only common name and unidentified) within the biodiversity plots.

	All trees recorded	Species identified	Only genus identified	Only family identified	Only common name	Unidentified
Absolute number	2733	2408	284	15	4	22
Percent (%)	100%	88%	10%	1%	0%	1%

All further analyses on tree community composition were conducted for lowland dipterocarp forest only. Mangrove was excluded as the variety of different tree species in the observed mangroves was very low (only up to six different tree species). Peat swamp forest was excluded because only three biodiversity plots were available and all were recorded after the fires of 2015.

Because some trees could not be identified to the species level all analyses on tree community composition are based on the genus level. Imai *at al.* (2014) showed that results on the genus level are highly correlated with those at the species level.

To assess the effects of different degradation levels on forest biodiversity the degree of similarity in tree community composition has gained increasing attention (Ioki *et al.* 2016, Barlow *et al.* 2007, Imai *et al.* 2012, Imai *et al.* 2014, Magurran and McGill 2011, Su *et al.* 2004, Ding *et al.* 2012). Nonmetric multidimensional scaling (nMDS) was applied to assess the differences in tree community composition among the biodiversity plots. The number of trees of each genus within the 38 biodiversity plots located in lowland dipterocarp forest was used as input to the Bray-Curtis similarity index to calculate the nMDS scores of axis 1 and axis 2. As there was no statistical significant correlation between forest density classes (Low-, Medium- and High-density Lowland Dipterocarp Forest) and the nMDS scores of axis 2, only scores from axis 1 very implemented in subsequent analyses. Further four biodiversity indices were calculated per biodiversity plot (Simpson index 1-D, Shannon index (entropy), Margalef's richness index and Equitability).

Results showed that there is a gradient in the mean nMDS axis 1 scores where Low-density Lowland Dipterocarp Forest with -0.214 had the lowest mean and High-density Lowland Dipterocarp Forest the highest with 0.109. Looking at the biodiversity indicators the two indices for 'richness/diversity' (Shannon index and Margelef's index) also had a similar gradient where the Low-density Lowland Dipterocarp Forest had the lowest and the High-density Lowland Dipterocarp Forest had the highest mean values indicating that High-density Lowland Dipterocarp Forest has the highest biodiversity. Also the other two biodiversity indicators for 'evenness' (Simpson index 1-D and Equitability) have a similar gradient which indicates that the High-density Lowland Dipterocarp Forest has the highest 'evenness' (all taxa are more equally present). All these findings indicate that high nMDS axis 1 scores go hand in hand with higher 'richness/diversity' and 'evenness'.

Next, to test whether there is a statistical significant difference between the different density classes (density stratification based on forest cover at 10 m height) with regard to nMDS and the biodiversity indicators a One-way ANOVA was performed. When the ANOVA results were significant, a Tukey's pairwise post-hoc test was used to identify the different pairs of groups. Results showed that there was a statistical significant ($p < 0.05$) difference between the means of the different density classes (Low, Medium and High) for the nMDS axis 1 scores, Shannon index and Margelef's index. Further, for all these three indicators the Tukey's pairwise post-hoc test showed there was a statistical significant ($p < 0.05$) difference between the density pairs Low vs Medium and Low vs High but not for Medium vs High. These statistical results indicate that there is a significant different with regard to tree community composition between these different density classes and that the density classes Low vs Medium and Low vs High could be best differentiated.

From the airborne LiDAR data 19 LiDAR metrics per biomass plot located within a LiDAR transect (n = 28) were derived. These LiDAR metrics were then correlated to the nMDS scores of axis 1 in order to derive a predictive LiDAR based tree community composition model. A stepwise forward and backward multiple regression was performed (R software was used for this). The final model included three significant variables (Mean, cov 12m = forest cover in percent at 12 m height and p 50^{th} = 50^{th} percentile) and four biodiversity plots were excluded (outliers) from the model development. An r^2 of 0.72 was obtained (n = 24).

This final model was then applied (spatial resolution 31.25 m) to the areas of the LiDAR transects that cover Lowland Dipterocarp Forest (based on the land cover classification from Work Package 2) (Figure 8). To exclude non-forested areas all areas where the LiDAR metric Max was smaller than 6 m were excluded. The predicted nMDS axis 1 scores of this map ranged from -0.264 to 0.741. The highest nMDS axis 1 scores were found in Kerinci Sebelat National Park and the lowest in eastern lowlands of the Musi Banyuasin district. These results indicate that the areas within the Kerinci Sebelat National Park have tree community compositions that indicate high biodiversity compared to the ones in the eastern lowlands of the Musi Banyuasin District.

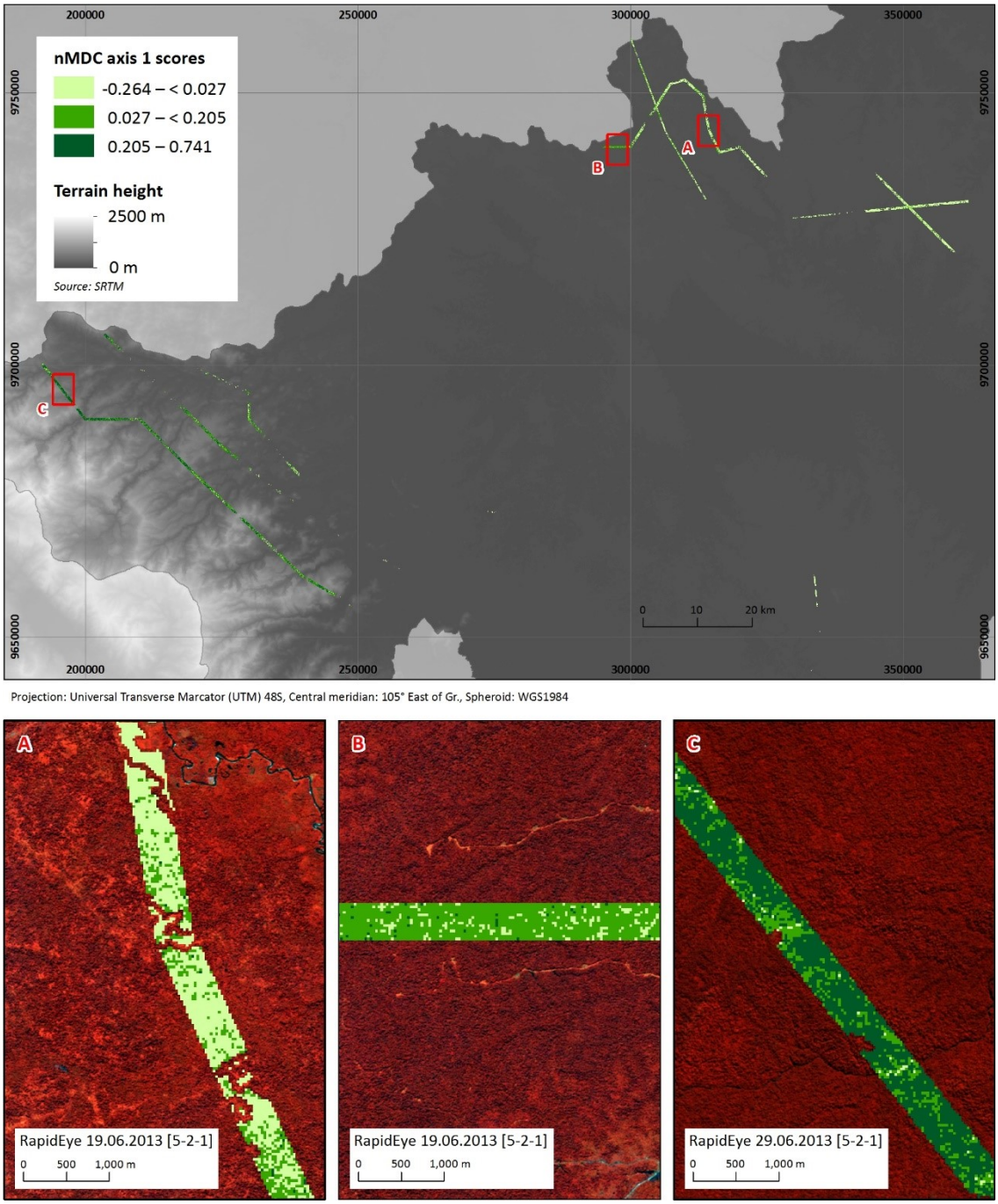

Figure 8: Final predictive LiDAR based tree community composition model. The predictive map shown here was reclassified into three classes using the Natural Breaks (Jenks) provided in ArcGIS (www.esri.com). The predicted nMDS axis 1 scores of this map ranged from -0.264 to 0.741. The lower three figures exemplarily show areas with low, medium and high nMDS axis 1 scores. The location of the lover three figures is shown as red rectangles in the upper figure. The highest nMDS axis 1 scores were found in Kerinci Sebelat National Park which indicates that this area has tree community compositions that indicate high biodiversity compared to the eastern lowland (e.g. District of Musi Banyuasin).

4.2. Work Package 1: Historic land cover change and carbon emission baseline

Figure 9 shows the flowchart of the activities carried out in Work Package 1 (WP 1): Historic land cover change and carbon emission baseline.

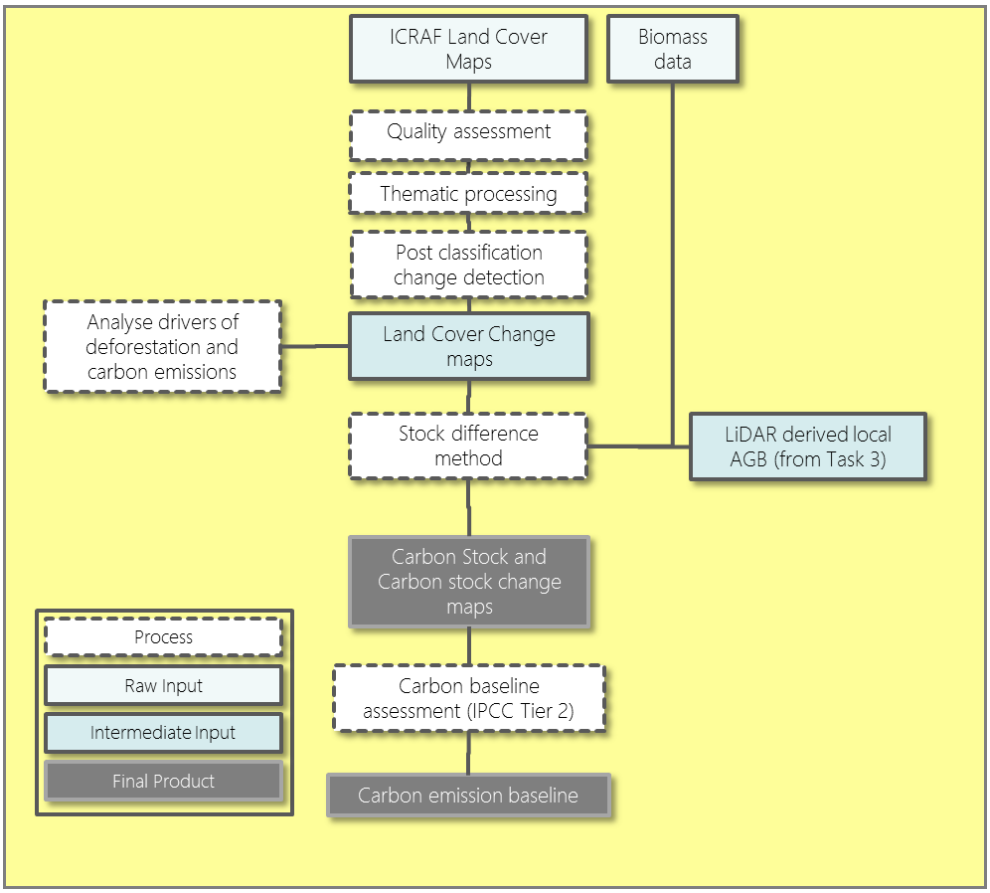

Figure 9: Flow chart of the activities carried out in Work Package 1 (WP 1): Historic land cover and carbon emission baseline.

4.2.1. Dataset

The assessment is based on the historic land cover data time series in the version 3 (framework of the project LAMA-I), as provided by ICRAF via ftp on 30 May 2016. A technical report which documents the methodology and results, and a dedicated report on the results of the accuracy assessment was received together with an earlier version of the dataset (Version 2). Table *7* shows the data available for this work package.

Table 7: Datasets provided by ICRAF

Filename	Type	Format
LC1990_v3_48s.tif	Raster	GeoTIFF
LC2000_v3_48s.tif	Raster	GeoTIFF
LC2005_v3_48s.tif	Raster	GeoTIFF
LC2010_v3_48s.tif	Raster	GeoTIFF
LC2014_v3_48s.tif	Raster	GeoTIFF
GPS_accuracy_all.shp	Point Vector	Shapefile
lc_legend.lyr	Symbology	Layerfile
lc_legend.xlsx	Spreadsheet	MS Excel
Accuracy_Assessment_result.docx	Report	MS Word
Technical report_LAMA-I_TZ_AP_VA_18062015.pdf	Report	PDF

A detailed technical assessment of the Version 2 of the data was conducted and the results are summarized in the internal report "Quality assessment report of ICRAF historic land cover change dataset". The report proved a very high quality of the analysis conducted, however, identified a variety of shortcomings of Version 2. As a consequence, a follow up Version 3 of the data was produced by ICRAF, and all shortcomings adequately addressed. Most importantly, the Version three was now delivered in full Landsat resolution of 30 meter which allows the exploitation of the data at maximum spatial scale.

4.2.2. Preprocessing

Before the land cover of the datasets could assessed different preprocessing steps had to be conducted in order to assure that the data in the correct format and all preconditions for a multi-temporal use of the data are met. Following preprocessing steps had to be carried out:

- Snap rasters: Raster files had to be brought into a common spatial grid in order to allow foe a multi-temporal overlay without spatial offset between the datasets.
- Conversion of the raster files into a polygon vector format (ESRI shapefile format)
- Verification of the class codes
- Generation of common spatial extent of the datasets
- Generation of a common no data mask (this step is necessary in order to facilitate the usability of the maps in terms of spatial extent, carbon storage and emissions)
- Conversion of the ICRAF classification scheme to the BAPLAN classification scheme (Figure 10)

ICRAF Code	ICRAF Classification Scheme	Translation	BAPLAN Classification scheme	Indonesian name	Baplan Code
1	Undisturbed forest	⟷	Primary dry land forest	Hutan lahan kering primer	2001
2	Logged over forest (High density)	⟷	Secondary/ logged over dry land forest	Hutan lahan kering sekunder/ bekas tebangan	2002
3	Logged over forest (Low density)	⟷			
4	Undisturbed swamp forest	⟷	Primary swawp forest	Hutan rawa primer	2005
6	Undisturbed peat swamp forest				
5	Logged over swamp forest	⟷	Secondary/ logged over swamp forest	Hutan rawa sekunder/ bekas tebangan	20051
7	Logged over peat swamp forest				
8	Undisturbed mangrove forest	⟷	Primary mangrove forest	Hutan mangrove primer	2004
9	Logged over mangrove forest	⟷	Secondary/ logged over mangrove forest	Hutan mangrove sekunder/ bekas tebangan	2007
10	Mixed garden	⟷	Mixed dryland agriculture/mixed garden	Pertanian lahan kering campur semak / kebun campur	20092
12	Coffee agroforest				
11	Rubber agroforest				
14	Oil palm monoculture	⟷	Tree crop plantation	Perkebunan/ Kebun	2010
15	Rubber monoculture				
16	Coconut monoculture				
13	Acacia plantation	⟷	Plantation forest	Hutan tanaman	2006
19	Shrub	⟷	Scrub	Semak belukar	2007
17	Rice field	⟷	Rice fields	Sawah/ persawahan	20093
18	Annual crops	⟷	Dry land agriculture	Pertanian lahan kering	20091
20	Grass	⟷	Grass	Rumput	3000
21	Cleared land	⟷	Open land	Tanah terbuka	2014
22	Settlement/Built-up area	⟷	Settlement/ developed land	Pemukiman/ lahan terbangun	2012
24	Waterbody	⟷	Water body	Tubuh air	5001
23	Fish pond	⟷	Embankment	Tambak	20094

Figure 10: Conversion key between the ICRAF classification scheme and the BAPLAN classification scheme.

4.2.3. Land cover

Figure 11 and Figure 12 exemplary show the land cover classification for the years 1990 and 2014. The spatial extent of the land cover classes for the years 1990, 2000, 2005, 2010 and 2014 is shown in Table 8.

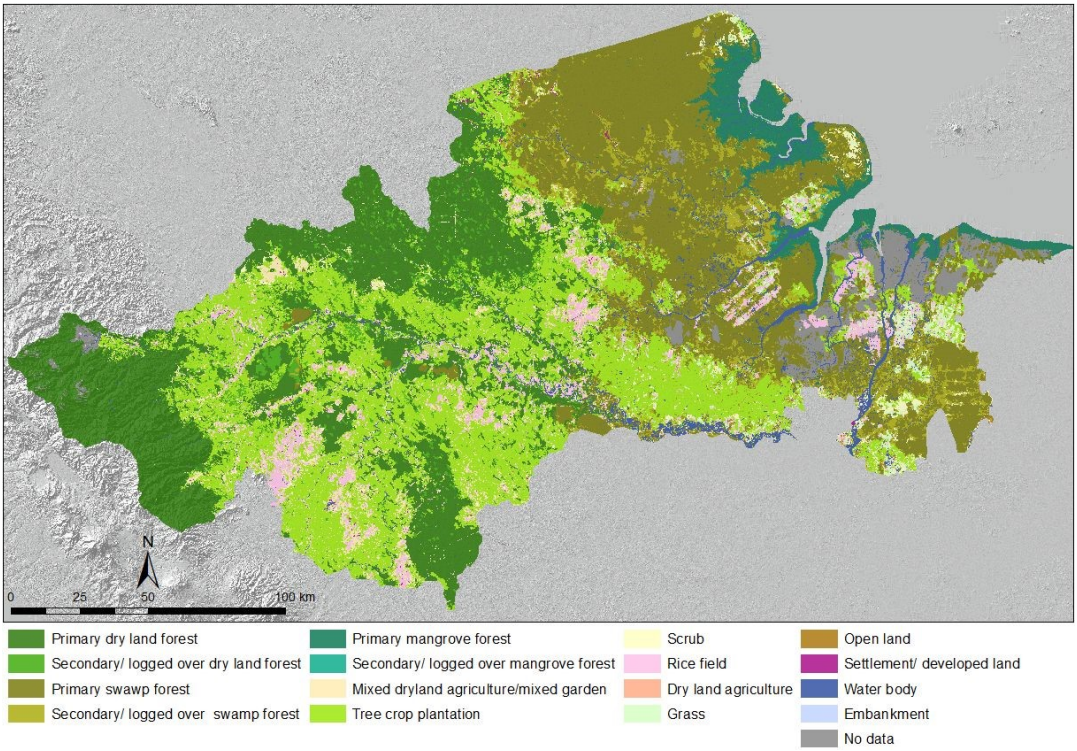

Figure 11: Land cover classification 1990.

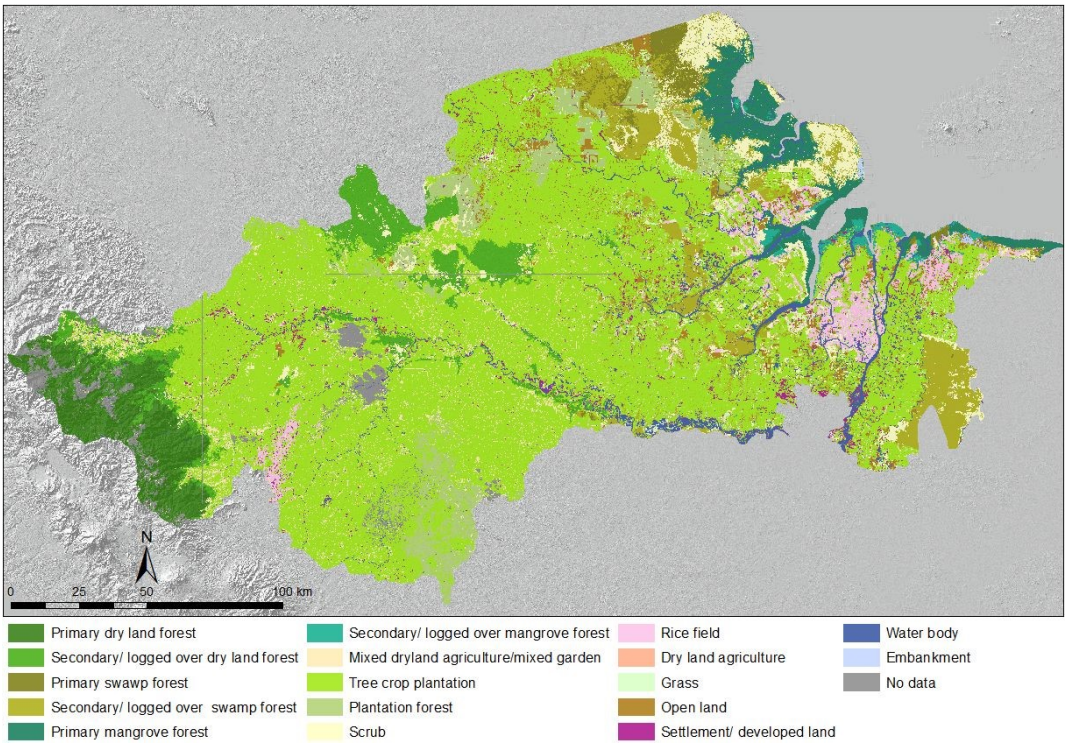

Figure 12: Land cover classification 2014.

Table 8: Spatial extent of the different land cover categories in the five points in time.

Land Cover	Area [ha]				
	1990	2000	2005	2010	2014
Primary dry land forest	871,563	289,632	260,314	193,063	171,254
Secondary/ logged over dry land forest	119,783	230,716	258,296	245,078	180,355
Primary swamp forest	859,638	397,310	256,148	167,487	47,206
Secondary/ logged over swamp forest	205,801	415,012	361,948	227,183	257,222
Primary mangrove forest	152,158	145,385	143,175	133,332	128,528
Secondary/ logged over mangrove forest	3,332	13,784	10,874	16,138	24,422
Mixed dryland agriculture/mixed garden	113,730	87,518	130,324	71,896	112,685
Tree crop plantation	1,007,473	1,348,775	1,675,992	1,954,907	2,075,566
Plantation forest	0	13,301	65,533	108,741	184,768
Scrub	68,633	99,263	99,247	101,408	177,000
Rice field	157,072	122,431	113,174	97,964	106,351
Dry land agriculture	3,453	7,109	13,391	32,236	1,629
Grass	48,768	26,898	14,206	63,618	45,259
Open land	6,395	28,996	22,220	12,524	93,848
Settlement/ developed land	7,909	11,722	19,034	28,494	58,899
Water body	109,532	109,526	109,526	109,532	109,532
Embankment	10	1,238	3,079	2,844	6,411
No data	129,469	516,101	308,239	298273.23	83,783
Sum	**3,864,718**	**3,864,718**	**3,864,718**	**3,864,718**	**3,864,718**

It has to be note that the maps and statistics above show the land cover status before the application of the common No data mask. The spatial extent of the land cover classes after the application of the common no data mask is shown in Table 9. These statistics form the basis for all further calculation of land cover changes and carbon emissions.

Table 9: Spatial extent of the different land cover categories after applying the common no data mask.

Land Cover	Area [ha]				
	1990	2000	2005	2010	2014
Primary dry land forest	535,947	249,237	228,878	176,525	171,254
Secondary/ logged over dry land forest	86,219	211,542	173,755	178,190	136,500
Primary swamp forest	626,024	308,027	225,233	167,409	47,206
Secondary/ logged over swamp forest	156,004	279,509	280,437	187,474	189,734
Primary mangrove forest	145,296	140,039	139,139	133,332	128,528
Secondary/ logged over mangrove forest	2,597	6,654	6,781	11,420	13,579
Mixed dryland agriculture/mixed garden	54,025	66,681	86,243	46,081	75,986
Tree crop plantation	848,023	1,162,293	1,267,981	1,432,675	1,461,231
Plantation forest	0	13,301	34,243	56,704	107,682
Scrub	39,038	63,508	66,113	65,004	103,395
Rice field	99,119	90,402	86,901	77,084	72,310
Dry land agriculture	2,443	6,077	7,864	25,926	1,187
Grass	38,081	16,209	9,296	50,598	30,296
Open land	4,645	19,353	13,664	10,121	57,574
Settlement/ developed land	6,999	11,111	16,912	24,536	44,390
Water body	109,526	109,526	109,526	109,526	109,526
Embankment	10	529	1,030	1,392	3,619
Sum	**2,753,996**	**2,753,996**	**2,753,996**	**2,753,996**	**2,753,996**
No data	1,110,722	1,110,722	1,110,722	1,110,722	1,110,722
Total	**3,864,718**	**3,864,718**	**3,864,718**	**3,864,718**	**3,864,718**

The most dominant land cover type in the study area was and is Tree crop plantation, occupying 848,023 ha in 1990 and expanding to 1,461,231 ha by 2014. The most abundant forest type in 1990 was Primary dryland forest with 535,947 ha, however this class lost about 68 % of its spatial extent until 2014 ending at 171,254 ha. Secondary dryland forest increased from 86,219 ha in 1990 to 211,542 ha in 2000, before decreasing until 2014. Primary peat swamp forest lost even more of its spatial extent, covering 626,024 ha in 1990, but only 47,206 ha in 2014. Large shares of these changes were due to forest degradation related to logging which is reflected by the increase of spatial extent of the Secondary/ logged over peat swamp forest. Most non forest classes experienced an increase in spatial extent, especially the plantation forest class, the mixed dryland agriculture class as well as the Settlement/ developed land class. A decrease in spatial extent was observed for the Rice field class.

4.2.4. Land cover change

Figure 13 exemplary show the land cover change between the years 1990 and 2014. The change in spatial extent for the different land cover classes is shown in Table 10. As already indicated in the previous chapter the most intensive losses in spatial extent were observed for the classes Primary dryland forest and Primary peatland forest, amounting to -364,692 ha and -578,818 ha in the overall observation period 1990 – 2014, respectively. The highest increase in spatial extent was observed in the Tree crop plantation class, amounting to 613,208 ha, followed by Plantation forest with 107,682 ha in the period 1990 – 2014.

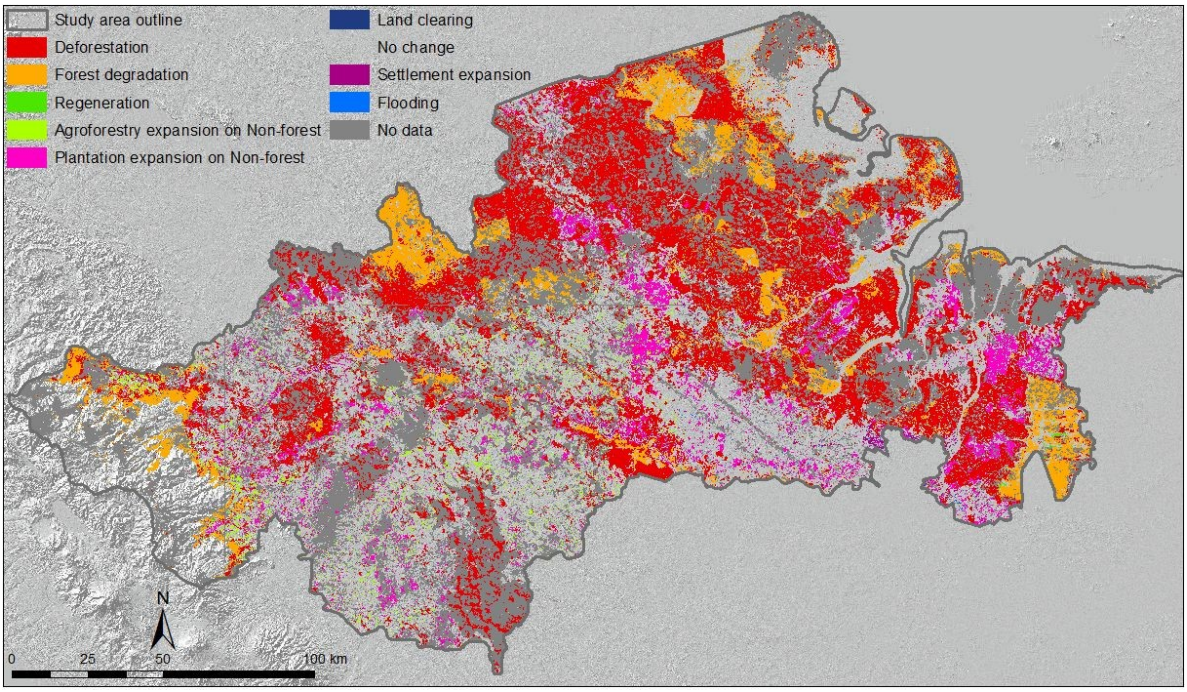

Figure 13: Land cover change 1990 – 2014.

Table 10: Land cover change in the five observation periods.

Land Cover	Area change (ha)				
	1990 - 2000	2000 - 2005	2005 - 2010	2010 - 2014	1990 - 2014
Primary dry land forest	-286,710	-20,358	-52,353	-5,271	-364,692
Secondary/ logged over dry land forest	125,322	-37,787	4,435	-41,689	50,281
Primary swamp forest	-317,997	-82,794	-57,824	-120,203	-578,818
Secondary/ logged over swamp forest	123,504	928	-92,963	2,260	33,730
Primary mangrove forest	-5,257	-900	-5,808	-4,804	-16,768
Secondary/ logged over mangrove forest	4,057	127	4,639	2,158	10,981
Mixed dryland agriculture/mixed garden	12,656	19,561	-40,161	29,904	21,960
Tree crop plantation	314,269	105,688	164,694	28,557	613,208
Plantation forest	13,301	20,942	22,460	50,978	107,682
Scrub	24,470	2,605	-1,109	38,391	64,357
Rice field	-8,717	-3,501	-9,817	-4,773	-26,808
Dry land agriculture	3,634	1,787	18,062	-24,739	-1,256
Grass	-21,872	-6,913	41,302	-20,302	-7,785
Open land	14,707	-5,689	-3,543	47,453	52,928
Settlement/ developed land	4,112	5,802	7,624	19,854	37,391
Water body	0	0	0	0	0
Embankment	519	500	363	2,227	3,608
Sum	**0**	**0**	**0**	**0**	**0**

Table 11 and Figure 14 present a summary of the spatial extent of the different land cover change processes and the importance of those across the five observation periods. The importance of those changed intensively across time: While in the first period 1990 – 2000, deforestation and forest degradation were almost equal in importance (accounting for 43% and 39% of all observed changes), degradation declined to between 13 and 18% in the following periods. The reason is that apart from areas with a strict protection status (such as the National parks), the majority of primary forest have already experienced degradation in the earliest observation period. At the same time, Plantation expansion on Non-forest increased significantly from 14% (1990 – 2000) to approximately 29 – 31% in the following periods. In the overall observation period 1990 – 2014, deforestation accounted for 63% of all observed changes, forest degradation for 20%, Plantation expansion on Non-forest for 12% and Agroforestry expansion on Non-forest for 3.5%.

Table 11: Spatial extent of the gross land cover changes in the five observation periods.

Change process	1990 - 2000	2000 - 2005	2005 - 2010	2010 - 2014	1990 - 2014
	Ha	Ha	Ha	Ha	Ha
	%	%	%	%	%
Deforestation	359,174	142,904	204,449	168,093	868,082
	42.85%	36.74%	45.82%	37.38%	62.79%
Forest Degradation	326,720	57,921	78,060	59,842	275,702
	38.98%	14.89%	17.50%	13.31%	19.94%
Plantation expansion on Non-forest	119,650	121,109	127,230	142,116	164,273
	14.27%	31.14%	28.52%	31.60%	11.88%
Regeneration	2,094	2,120	4,576	544	2,796
	0.25%	0.55%	1.03%	0.12%	0.20%
Settlement expansion	2,524	4,951	5,354	17,894	21,851
	0.30%	1.27%	1.20%	3.98%	1.58%
Land clearing	449	419	135	1,277	340
	0.05%	0.11%	0.03%	0.28%	0.02%
Agroforestry expansion on Non-forest	27,510	59,052	25,992	57,667	47,596
	3.28%	15.18%	5.83%	12.82%	3.44%
Flooding	155	462	377	2,289	1,844
	0.02%	0.12%	0.08%	0.51%	0.13%
Total Changes	**838,273**	**388,938**	**446,173**	**449,722**	**1,382,485**
No Change	**1,915,723**	**2,365,058**	**2,307,823**	**2,304,273**	**1,371,511**
Total	**2,753,996**	**2,753,996**	**2,753,996**	**2,753,996**	**2,753,996**

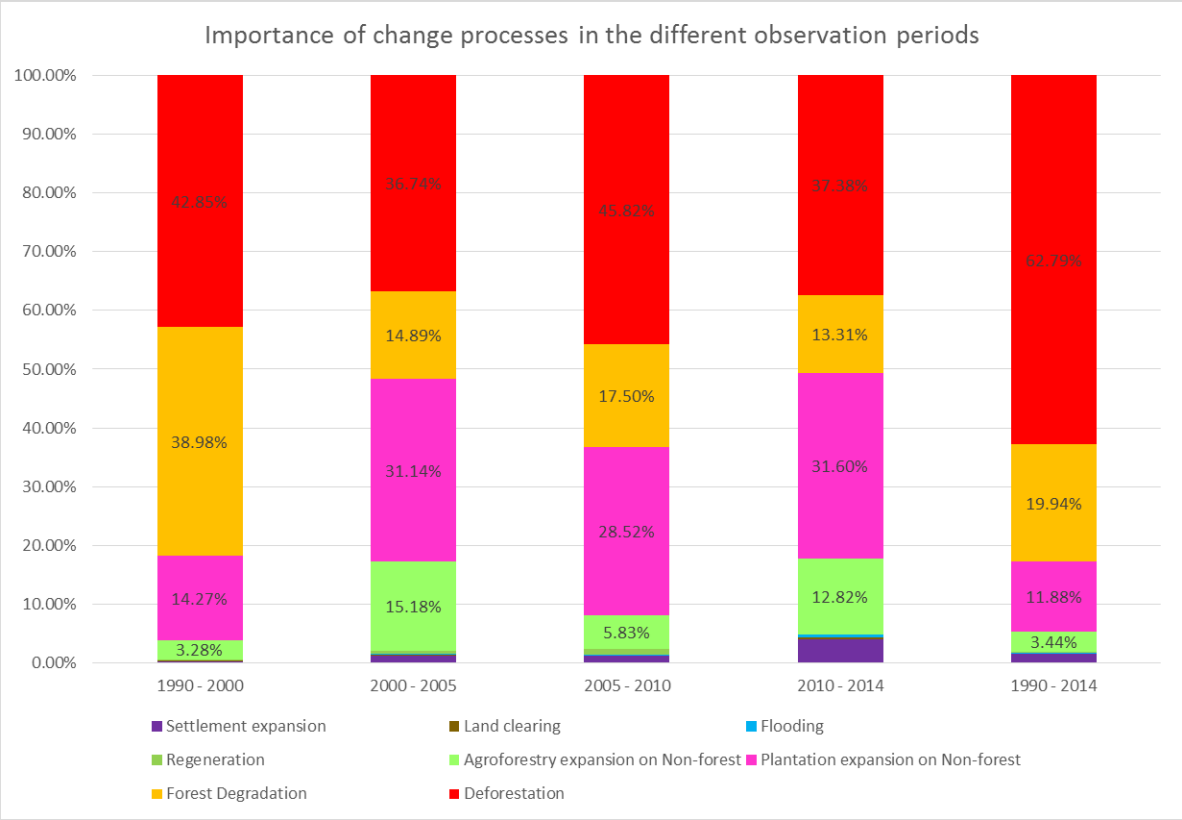

Figure 14: Importance of change processes in the different observation periods.

4.2.5. Deforestation rate

Table 12 shows the net forest losses in the five observation periods. Between 1990 and 2000, 357,080 ha of forest have been lost which amounts to 23% of the forest cover at the start of the observation period. In the following periods, another 140,784 ha (12%), 199,873 ha (19%) and 167,549 ha (20%) have been lost. In the overall observation period 1990 – 2014, net forest loss amounted to 865,286 ha or 56% of the forest cover of 1990.

Table 12: Net forest loss in the five observation periods.

Net forest loss	1990 - 2000	2000 - 2005	2005 - 2010	2010 - 2014	1990 - 2014
ha	-357,080	-140,784	-199,873	-167,549	-865,286
%	-23.01%	-11.78%	-18.96%	-19.61%	-55.75%

Figure 15 shows the resulting annual deforestation rates in the study area in the five observation periods. It is interesting to note that the deforestation rates increased over time. While between 1990 and 2000, approx. 2.3% of forest cover have been lost annually, this rate increased in the following periods up until 4.9% per year. The reason is that while net forest loss remained on a more or less constant level (with a peak between 2005 and 2010), the spatial extent of forest cover diminished significantly. Therefore, the relative rates increase over time. In the overall observation period 1990 – 2014 the annual deforestation rate averaged at 2.3%.

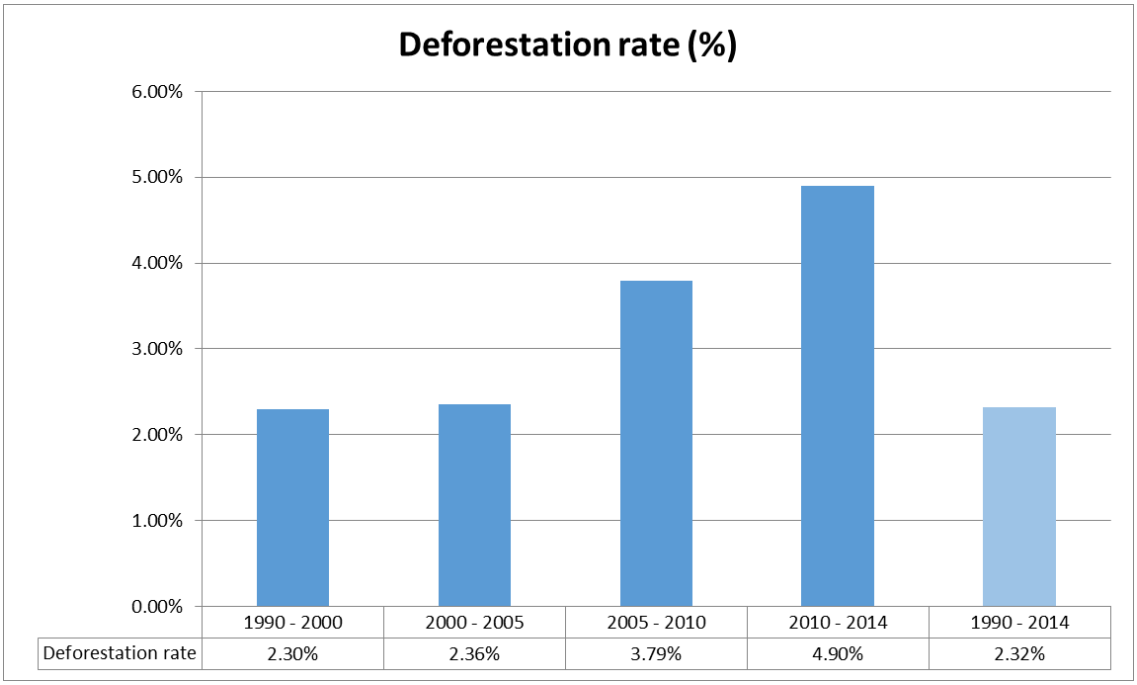

Figure 15: Annual deforestation rate in the five observation periods.

Figure 16 shows the analysis of deforestation drivers across the five observation periods. These varied significantly over time. While conversion to tree crop plantation remained the most important driver, its importance first increased from 67% between 1990 and 2000 to 73% between 2000 and 2005, before it started to decrease to 62% (2005 – 2010) and then to 43% (2010 – 2014). Overall, conversion to tree crop plantation accounted for 65% of all deforestation between 1990 and 2014. The second most important driver of deforestation over time was conversion to Scrub, which accounted for 9% (1990 – 2000), 6% (2000-2005), 10 % (2005 – 2010) and 25% (2010 – 2014) of all deforestation. Conversion to plantation forest accounted for 2.5% (1990 – 2000), 2.3% (2000 – 2005), 2.6% (2005 – 2010) and 14% (2010 – 2014). In the overall period 1990 – 2014, this conversion amounted for almost 10% of all deforestation. Less important drivers of deforestation in the overall period 1990 – 2014 were Conversion to Open land (5%), Conversion to Rice field (4%) and Conversion to mixed dryland agriculture (3%).

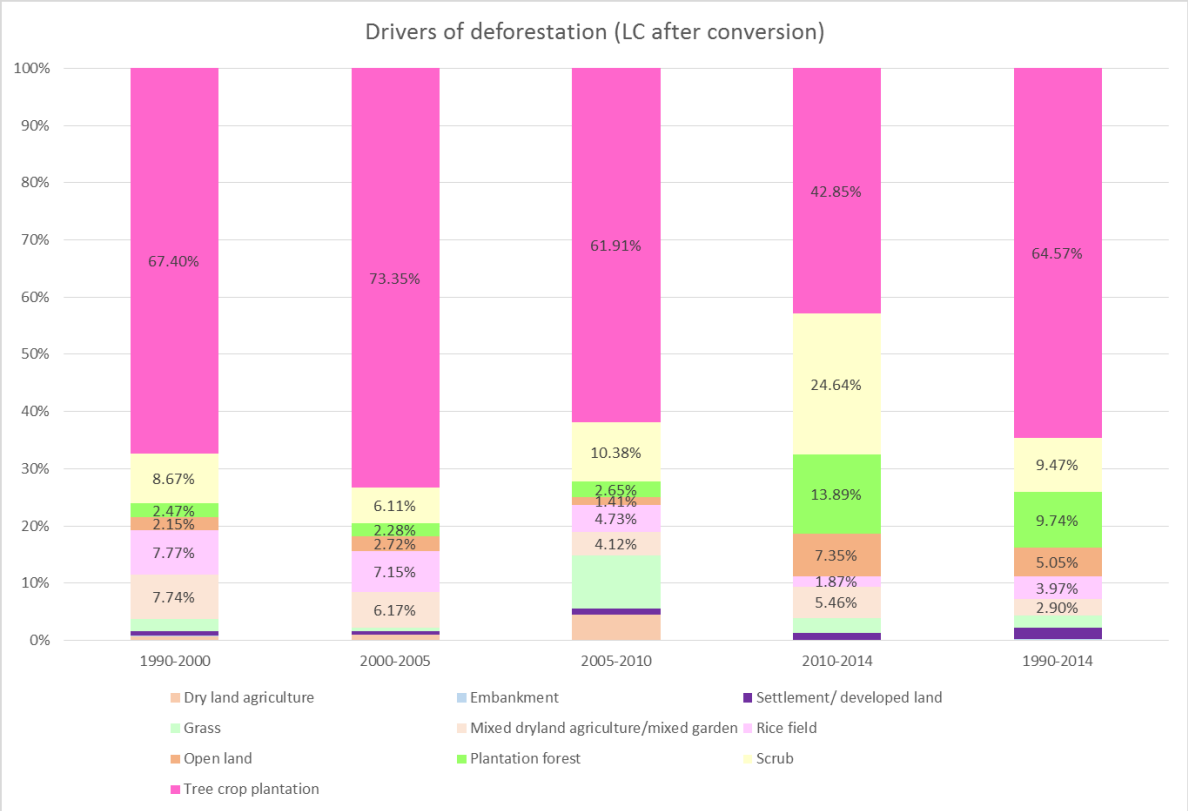

Figure 16: Drivers of deforestation.

4.2.6. Carbon stock

To derive the carbon stock maps, the local aboveground biomass values derived in Work Package 3 (WP 3) were attributed to the different land cover classes. Carbon stock is reported in tons of carbon (t C). To calculate the carbon content of a certain stratum, the aboveground biomass value is simply divided by 2 (i.e. a carbon content of 0.5 is assumed). By multiplying the extent of the land cover by the carbon content per hectare per land cover class the total carbon stock of the respective land cover class is calculated (stratify & multiply approach).

Figure 17 and Figure 18 exemplary show the carbon stock maps for the years 1990 and 2014. The carbon stock of the land cover classes for the years 1990, 2000, 2005, 2010 and 2014 is shown in Table 13.

The majority of carbon was and is stored in the classes primary dryland forest amounting to 146,045,443 t C in 1990 and still 46,666,832 t C in 2014. The second highest carbon stock was observed in Primary peat swamp forest in 1990 with 70,740,679 t C, however, this declined to only 5,334,226 t C in 2014. Carbon storage in Primary mangrove forest remained almost constant over time. Carbon stocks in the secondary forest lasses (Dry land and Swamp) increased at first, but then decreased as well due to deforestation of secondary forests over time.

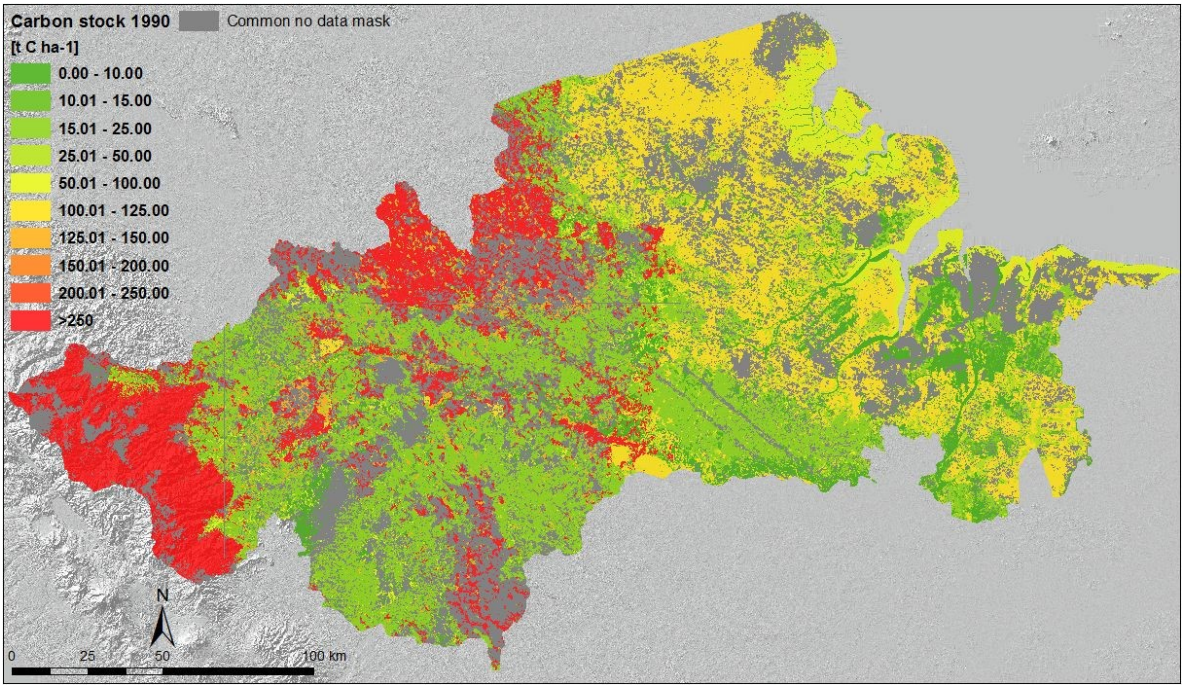

Figure 17: Carbon stock map 1990.

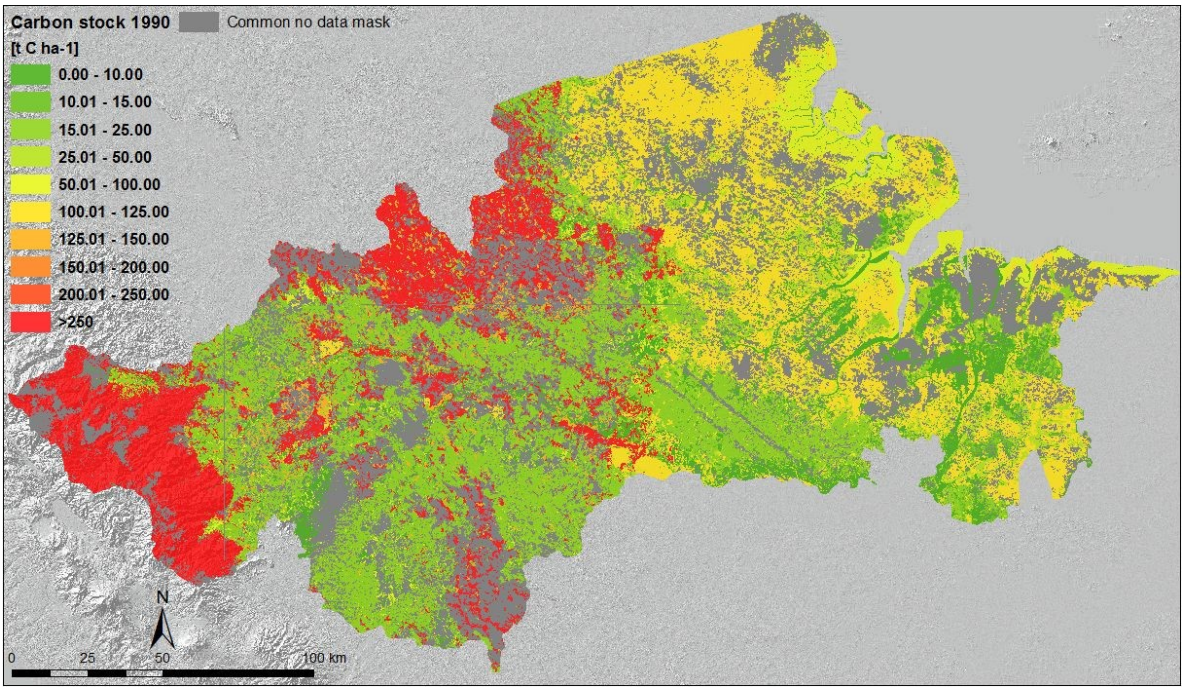

Figure 18: Carbon stock map 2014.

Table 13: Carbon stored in the different land cover classes at the five points in time.

Land Cover	Carbon stock (t C)				
	1990	2000	2005	2010	2014
Primary dry land forest	146,045,443	67,917,009	62,369,356	48,103,114	46,666,832
Secondary/ logged over dry land forest	11,036,091	27,077,322	22,240,581	22,808,287	17,472,038
Primary swamp forest	70,740,679	34,807,018	25,451,289	18,917,166	5,334,226
Secondary/ logged over swamp forest	5,772,165	10,341,828	10,376,160	6,936,543	7,020,166
Primary mangrove forest	14,384,304	13,863,889	13,774,807	13,199,862	12,724,300
Secondary/ logged over mangrove forest	57,139	146,393	149,191	251,250	298,729
Mixed dryland agriculture/mixed garden	2,836,328	3,500,771	4,527,736	2,419,276	3,989,247
Tree crop plantation	13,568,373	18,596,684	20,287,692	22,922,794	23,379,703
Plantation forest	0	266,013	684,860	1,134,070	2,153,637
Scrub	487,970	793,847	826,416	812,553	1,292,438
Rice field	495,594	452,011	434,506	385,418	361,552
Dry land agriculture	37,867	94,195	121,899	401,856	18,396
Grass	118,051	50,248	28,818	156,854	93,917
Open land	0	0	0	0	0
Settlement/ developed land	0	0	0	0	0
Water body	0	0	0	0	0
Embankment	0	0	0	0	0
Sum	**265,580,004**	**177,907,228**	**161,273,311**	**138,449,043**	**120,805,181**

4.2.7. Carbon stock change

Table 14 shows the carbon stock changes in the land cover classes across time. The most intensive carbon losses (in the overall observation period) were observed in Primary dryland forest amounting to -99,378,611 t C and in Primary swamp forest amounting to -65,406,453 t C. Compared to these enormous losses, the increases in carbon stock observed in the Tree crop plantation class (9,811,331 t C between 1990 and 2014) and Secondary dryland forest (6,435,948 t C) are considered minor.

Table 14: Carbon stock change in the five observation periods.

Land Cover	Carbon stock change (t C)				
	1990 - 2000	2000 - 2005	2005 - 2010	2010 - 2014	1990 - 2014
Primary dryland forest	-78,128,434	-5,547,653	-14,266,242	-1,436,282	-99,378,611
Secondary/ logged over dryland forest	16,041,231	-4,836,741	567,706	-5,336,248	6,435,948
Primary swamp forest	-35,933,661	-9,355,729	-6,534,123	-13,582,940	-65,406,453
Secondary/ logged over swamp forest	4,569,662	34,332	-3,439,617	83,623	1,248,001
Primary mangrove forest	-520,415	-89,082	-574,944	-475,562	-1,660,004
Secondary/ logged over mangrove forest	89,254	2,798	102,059	47,478	241,590
Mixed dryland agriculture/mixed garden	664,444	1,026,965	-2,108,460	1,569,971	1,152,919
Tree crop plantation	5,028,312	1,691,008	2,635,102	456,909	9,811,331
Plantation forest	266,013	418,847	449,210	1,019,567	2,153,637
Scrub	305,877	32,569	-13,863	479,886	804,468
Rice field	-43,583	-17,505	-49,087	-23,866	-134,042
Dryland agriculture	56,327	27,705	279,957	-383,460	-19,471
Grass	-67,803	-21,430	128,036	-62,937	-24,134
Open land	0	0	0	0	0
Settlement/ developed land	0	0	0	0	0
Water body	0	0	0	0	0
Embankment	0	0	0	0	0
Sum	**-87,672,776**	**-16,633,917**	**-22,824,268**	**-17,643,863**	**-144,774,823**

Annual carbon stock changes are shown in Table 15.

Table 15: Annual carbon stock change in the five observation periods.

Land Cover	Annual Carbon Emissions (t C yr-1)				
	1990 - 2000	2000 - 2005	2005 - 2010	2010 - 2014	1990 - 2014
Primary dry land forest	-7,812,843	-2,219,061	-2,853,248	-359,071	-4,140,775
Secondary/ logged over dry land forest	1,604,123	-1,934,696	113,541	-1,334,062	268,164
Primary swamp forest	-3,593,366	-3,742,292	-1,306,825	-3,395,735	-2,725,269
Secondary/ logged over swamp forest	456,966	13,733	-687,923	20,906	52,000
Primary mangrove forest	-52,042	-35,633	-114,989	-118,891	-69,167
Secondary/ logged over mangrove forest	8,925	1,119	20,412	11,870	10,066
Mixed dryland agriculture/mixed garden	66,444	410,786	-421,692	392,493	48,038
Tree crop plantation	502,831	676,403	527,020	114,227	408,805
Plantation forest	26,601	167,539	89,842	254,892	89,735
Scrub	30,588	13,027	-2,773	119,971	33,520
Rice field	-4,358	-7,002	-9,817	-5,967	-5,585
Dry land agriculture	5,633	11,082	55,991	-95,865	-811
Grass	-6,780	-8,572	25,607	-15,734	-1,006
Open land	0	0	0	0	0
Settlement/ developed land	0	0	0	0	0
Water body	0	0	0	0	0
Embankment	0	0	0	0	0
Sum	**-8,767,278**	**-6,653,567**	**-4,564,854**	**-4,410,966**	**-6,032,284**

Figure 19 shows the analysis of the drivers of carbon emissions, as derived from the carbon change matrices of the emission assessment. The driver analysis is based on the class into which the land cover was converted in the respective time period, and it shows the emissions (or removals) resulting from the conversion, as well as the source of the emissions (i.e. which class was converted and how large the emissions from this class are.

The highest emissions are caused by conversion into Tree crop plantation, accounting for almost 80 million tons of carbon emissions in the time period 1990 – 2014. The majority of those emissions (45 million t C) come from the conversion of Primary dryland forest, followed by approx. 25 million t C from the conversion of Primary peat swamp. The second highest emissions were caused by logging of primary dryland forest, amounting to 16 million t C, followed by the conversion to Plantation forest amounting to approx. 13 million t C. Logging of primary swamp forest caused another 11 million t C emissions.

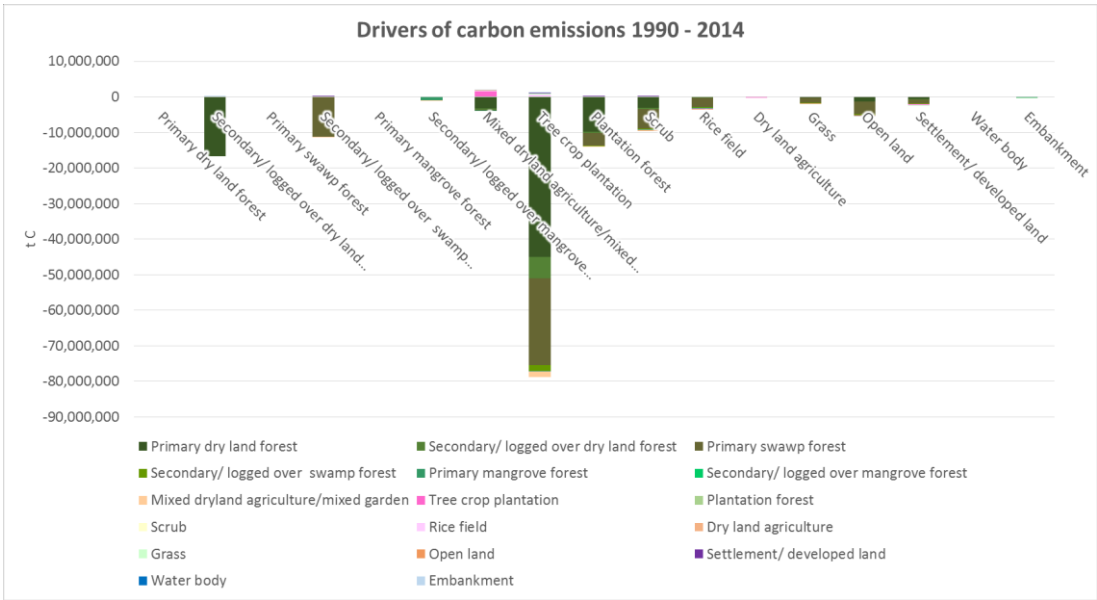

Figure 19: Drivers of carbon emissions.

4.2.8. Carbon emission baseline

Based on the carbon stock maps and the carbon stock statistics for the five points in time, a simple carbon emission baseline assessment was conducted. The baseline shown in Figure 20 is a simple mathematical projection of the carbon stock into the future by a logarithmic trend function. The prediction was made until the year 2014. Projected carbon stock for 2014 is approximately 75,000,000 t C, i.e. predicted emissions in the next 50 years amount to approximately 50,000,000 t C. It has to be noted that this business-as-usual scenario is solely a mathematical projection of the historic trend in total carbon stock, and does not consider any other variables.

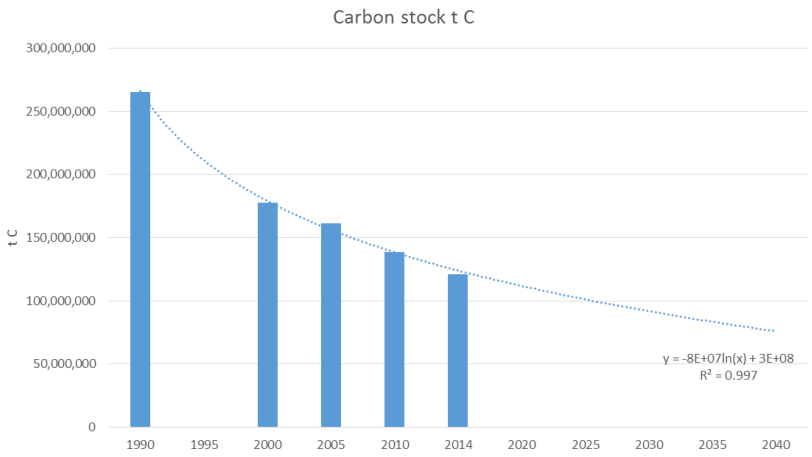

Figure 20: Development of total carbon stocks over time and carbon emission baseline.

4.3. Work Package 2: Forest benchmark mapping and monitoring

Figure 21 shows the flowchart of the activities carried out in Work Package 1 (WP 1): Historic land cover change and carbon emission baseline.

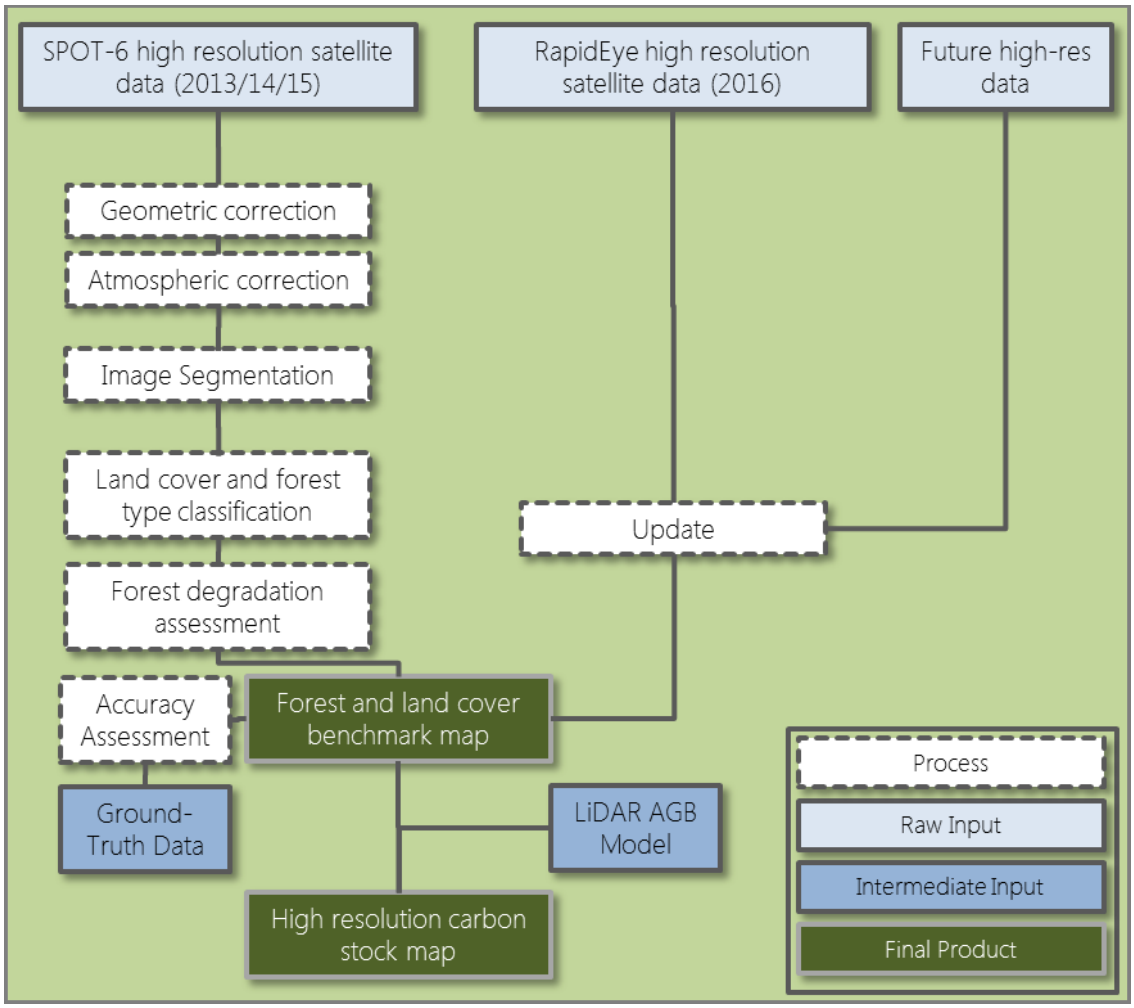

Figure 21: Flow chart of the activities carried out in Work Package 2 (WP 2): Forest benchmark mapping and monitoring.

4.3.1. Dataset

Because it was not possible to cover the whole project area by SPOT images, it was necessary to acquire additional data with similar spectral and spatial characteristics. On this account also RapidEye data was used for generating the benchmark maps.

The update of the map (Time step 2) was mostly done using RapidEye data from 2016. Anyway because of bad weather conditions with an almost cloudy sky in 2016 it was not possible to cover all project areas with high resolution images. So it was decided to use Landsat 8 data to fill these missing parts. This way allows a founded analysis of land cover change also in areas without RapidEye data.

4.3.2. Preprocessing

The first step of the preprocessing was the geometric correction of the used SPOT-6 and RapidEye images. A geometric correction including orthorectification of the images was carried out based reference ground control points derived from the aerial photos collected during the LiDAR survey in October 2014 (which was referenced to a network of benchmarks of the Indonesian Geodetic Agency BIG) and Landsat satellite imagery (which was used in the historic land cover assessment by ICRAF). In order to apply terrain rectification, the digital elevation model (DEM) from the Shuttle Radar Topography Mission (SRTM) with a global resolution of 30 m was used. Based on the RPCs of the imagery, the GCPs and the DEM, a sensor specific model for SPOT-6 and RapidEye was used for geometric correction in the software ERDAS Imagine 2014.

The second step of the pre-processing was the removal of atmospheric distortions (scattering, illumination effects, adjacency effects), induced by water vapor and aerosols in the atmosphere, seasonally different illumination angles etc. An atmospheric correction was applied to each image using the software ATCOR (Richter and Schläpfer 2014).

4.3.3. Land cover

The satellite images were then used as input to land cover classification using an object-based image analysis. This methodology classifies spatially adjacent and spectrally similar groups of pixels, so called image objects, rather than individual pixels.

Based on the national forest definition of Indonesia and the land cover classification scheme used by BAPLAN, one land cover classification scheme was designed (Table 16).

Table 16: Classification scheme

BAPLAN Classification scheme	Indonesian name	BAPLAN Code	BIOCLIME class	BAPLAN-enhanced code
Primary dry land forest	Hutan lahan kering primer	2001	High-density Lowland Dipterocarp Forest	2001-1
			High-density Lower Montane Rain Forest	2001-2
			High-density Upper Montane Rain Forest	2001-3
Secondary/ logged over dry land forest	Hutan lahan kering sekunder/ bekas tebangan	2002	Medium-density Lowland Dipterocarp Forest	2002-1
			Low-density Lowland Dipterocarp Forest	2002-2
			Medium-density Lower Montane Rain Forest	2002-3
			Low-density Lower Montane Rain Forest	2002-4
			Medium-density Upper Montane Rain Forest	2002-5
			Low-density Upper Montane Rain Forest	2002-6

BAPLAN Classification scheme	Indonesian name	BAPLAN Code	BIOCLIME class	BAPLAN-enhanced code
Primary swamp forest	Hutan rawa primer	2005	High-density peat swamp forest	2005-1
			Permanently inundated peat swamp forest	2005-2
			High-density back swamp forest	2005-3
			High-density freshwater swamp forest	2005-4
			Heath forest	2005-5
Secondary/ logged over swamp forest	Hutan rawa sekunder/ bekas tebangan	20051	Medium-density peat swamp forest	20051-0
			Low-density peat swamp forest	20051-1
			Regrowing peat swamp forest	20051-2
			Low-density back swamp forest	20051-3
			Regrowing back swamp forest	20051-4
			Medium-density Freshwater Swamp Forest	20051-5
			Low-density Freshwater Swamp Forest	20051-6
Primary mangrove forest	Hutan mangrove primer	2004	Mangrove 1	2004-1
			Mangrove 2	2004-2
			Nipah Palm	2004-3
Secondary/ logged over mangrove forest	Hutan mangrove sekunder/ bekas tebangan	9999	Degraded mangrove	2007-1
			Young mangrove	2007-2
Mixed dryland agriculture/mixed garden	Pertanian lahan kering campur semak / kebun campur	20092	Dryland agriculture mixed with shrub	20092-1
			Rubber agroforestry	20092-2
Tree crop plantation	Perkebunan/ Kebun	2010	Oil palm plantation	2010-1
			Coconut plantation	2010-2
			Rubber plantation	2010-3
Plantation forest	Hutan tanaman	2006	Acacia plantation	2006-1
			Industrial forest	2006-2
Scrub	Semak belukar	2007	Scrubland	2007
Swamp scrub	Semak belukar rawa	20071	Swamp scrub	20071
Rice fields	Sawah/ persawahan	20093	Rice field	20093
Dry land agriculture	Pertanian lahan kering	20091	Dry land agriculture	20091

BAPLAN Classification scheme	Indonesian name	BAPLAN Code	BIOCLIME class	BAPLAN-enhanced code
Grass	Rumput	3000	Grassland	3000
Open land	Tanah terbuka	2014	Bare area	2014
Settlement/ developed land	Pemukiman/ lahan terbangun	2012	Settlement	2012-1
			Road	2012-2
Water body	Tubuh air	5001	Water	5001
Swamp	Rawa	50011	Wetland	50011
Embankment	Tambak	20094	Aquaculture	20094

A field survey was conducted in 2015 to assess the accuracy of the land cover and forest benchmark map, as well as the forest degradation information. This included collecting vegetation type and height, canopy cover and further information at 373 sampling sites. Ground truth data was also collected during a field survey in 2016, and used to validate the maps from time step 2. Data on a further 429 sampling locations was documented during this time. All field samples were collected in accordance with the FAO Land Cover Classification System (LCCS) and the class hierarchy designed for BIOCLIME.

General guidelines for large areas (more than about 400,000 ha) suggest, that a minimum of 75 samples should be taken per category or land cover class (Congalton and Green 2008). Together, the classified BIOCLIME districts have a spatial extent of more than 1,000,000 ha and span 17 land cover classes (according to the BAPLAN classification scheme). As a result, it was necessary to supplement the field-based ground truth data with further reference data.

In the case of the benchmark map, this was accomplished by interpreting aerial photos (acquired in 2014) with very fine spatial resolution. In order to guarantee a statistically representative validation dataset and taking time and budget into consideration, it was decided that a further 1,127 reference polygons would be derived using this method.

To ensure adequate validation of the updated map, orthomosaics collected by a UAV were used in the same fashion as the aerial photos used for time step 1. This data was acquired as part of the field survey in 2016. Additional RapidEye images which were not used for classification were also used for validation purposes. In total, 217 reference polygons generated from UAV data and 759 taken from independent RapidEye images were used to validate the maps for time step 2.

All polygons incorporated into the validation were selected by random sampling within the aerial photo transects, the UAV orthomosaics and the unused RapidEye images. This method ensures that each sample unit in the study area has an equal chance of being selected. The advantage of this approach is that it minimizes bias and is assumed to deliver representative results.

Based on these reference data through an accuracy matric the respective user and producer accuracies, overall accuracy and the Kappa index were calculated.

Classifying according to the BAPLAN classification scheme produced an overall accuracy of 84.4% and a Kappa index of 0.83 for Time Step 1 (2014). For Time Step 2 (2016) an overall accuracy of 87% and a Kappa index of 0.86 was reached.

Table 17 and Figure 22 to Figure 23 exemplarily show the land cover classification results for the Kerinci Seblat National Park project site. A detailed description of all land cover results for all nine project areas can be found in the final report for Work Package 2 (WP 2).

Table 17: Spatial extent of the land cover classes for the years 2014 and 2016 for Kerinci Seblat national Park project site.

Class name	2014		2016	
	Area (ha)	%	Area (ha)	%
High-density lowland dipterocarp forest	47,733	18.5	43,262	16.7
High-density lower montane rain forest	20,515	7.9	21,601	8.4
High-density upper montane rain forest	2,017	0.8	2,567	1.0
Medium-density lowland dipterocarp forest	65,107	25.2	64,207	24.9
Low-density lowland dipterocarp forest	17,048	6.6	15,917	6.2
Medium-density lower montane rain forest	5,442	2.1	5,345	2.1
Low-density lower montane rain forest	631	0.2	617	0.2
Medium-density upper montane rain forest	-	-	12	0.0
Low-density upper montane rain forest	17	0.0	17	0.0
Dryland agriculture mixed with shrub	2,422	0.9	11,770	4.6
Oil palm plantation	5	0.0	156	0.1
Rubber Agroforestry	62,224	24.1	59,845	23.2
Scrubland	17,041	6.6	16,123	6.2
Dryland agriculture	6,573	2.5	2,025	0.8
Bare area	497	0.2	730	0.3
Settlement	402	0.2	438	0.2
Road	152	0.1	190	0.1
Water	2,066	0.8	2,048	0.8
Wetland	9	0.0	13	0.0
NoData	8,398	3.3	11,415	4.4
	258,299	**100.0**	**258,299**	**100.0**

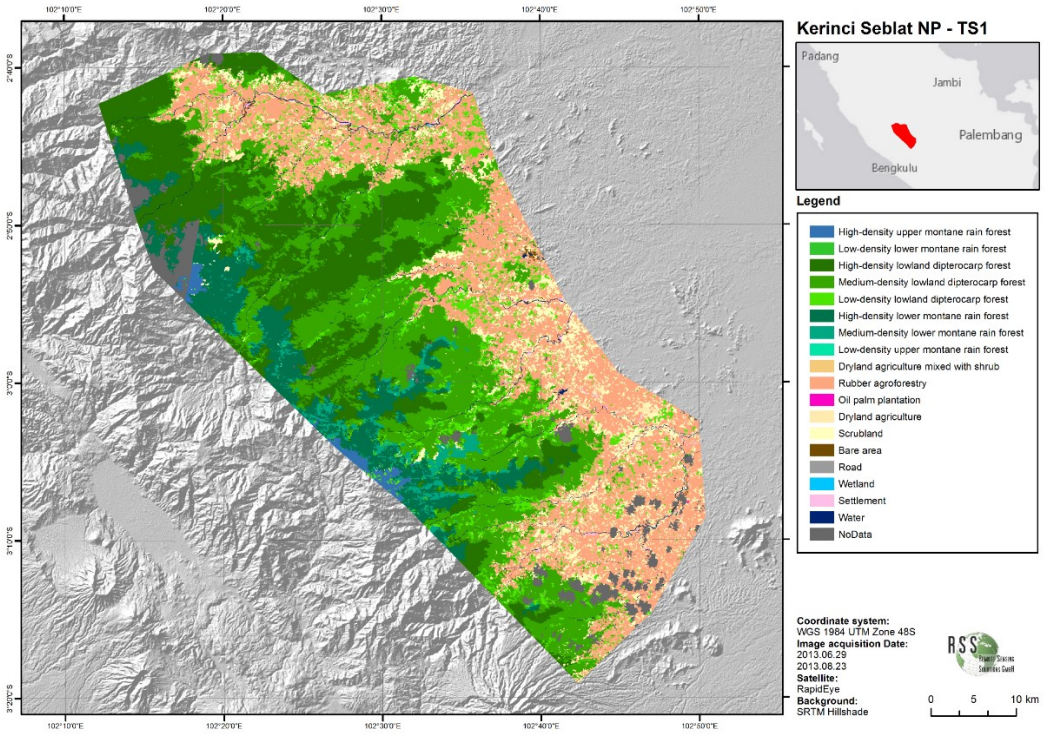

Figure 22: Land cover map of Kerinci Seblat National Park project site for time step 2014.

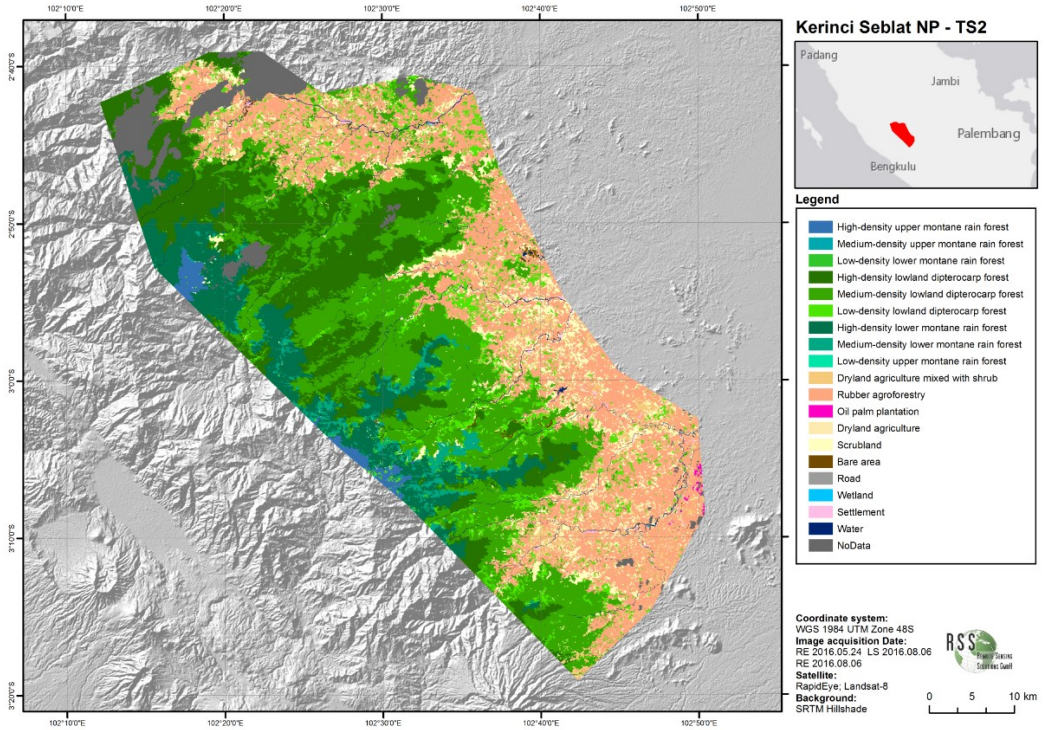

Figure 23: Land cover map of Kerinci Seblat National Park project site for time step 2016.

4.3.4. Land cover change

The analysis of all possible changes between the benchmark - and the updated map shows in this case a possibility of 1936 change vectors. So similar to the change analysis based on ICRAF classifications, groups of several change vectors into meaningful classes where created. Table 18 and Figure 24 show a detailed breakdown of the changes by project area. Here also common No Data areas were considered. A detailed description for each project site can be found in the final report to Work Package 2.

Of the eight processes observed, deforestation was by far the most dominant. A minimum of 12.8% (Benakat) and as much as 86.6% of change in each project area was attributed to deforestation. Deforestation was strongest in Sembilang and Lalan, where 21,214 ha (86.6%) and 53,065 ha (86.1%) of forests were cleared respectively. Conversely, Benakat and Dangku experienced the least deforestation, losing 456 ha and 748 ha of forest respectively. Although these two regions lost the least amount of forested area, deforestation explains approximately one third (29.9%) of the changes that occurred in Dangku but only 12.8% of changes in Benakat.

Sembilang and Lalan cleared the most forest but other regions saw higher rates of forest degradation. Reki lost less than one sixth of the forest removed in Sembilang but degraded almost ten times (3,895 ha) more than Sembilang. Mangrove and Benakat experienced the least forest degradation while 1,645 ha were degraded in Dangku, amassing to 65.7% of all changes observed there. Although 41.7% of changes were attributed to deforestation, the highest proportion of changes in Mangrove occurred due to agricultural expansion on non-forest. This change in Mangrove (43.7%, or 5.594 ha) is more than five times greater than the next highest region (965 ha accounting for 27% of change in Benakat). In contrast, Dangku and Reki experienced the least agricultural expansion, converting 34 and 44 hectares of non-forest to agriculture respectively. Change in Reki was also only 0.6% due to agricultural expansion.

Reki also saw the least amount of plantation expansion onto non-forest (1.7% or 136 ha) with respective to total change. In terms of total area, however, Dangku converted the least non-forest to plantation (46 ha). The most plantation expansion by area was documented in Lalan (2,757 ha) but this contributed to a mere 4.5% of changed in the project area. Benakat and Lakitan converted approximately half the amount of non-forest to plantation (1.902 and 1,200 ha respectively) but found this process to be one of the leading causes of change in the region, explaining 53.3% of differences in Benakat and 20.9% of change in Lakitan. The final variation of expansion assessed – settlement expansion – consistently described less than 0.3% of changes in any given study area. Settlements grew the most in Mangrove, where 44 hectares of land changed to settlement, and saw no change in five (Bentayan, Dangku, Lakitan, Lalan, Reki) of the nine regions.

Flooding similarly influenced very little of the changes documented but occurred consistently in each region other than Benakat. Sembilang was the most affected by flooding, where 280 hectares of dry land became wetted. Nevertheless, this change only accounts for 1.1% of all changes in Sembilang. Sembilang also cleared the second largest area of land (622 ha), surpassing all other regions but Lalan, where 790 ha were cleared. These changes describe less than 2.5% of changes in each aforementioned region, however, and explain up to 6.2% of the changes that took place in Benakat. Benakat also revitalized the least amount of land in terms of area (16 ha), and Lalan regenerated the most (2,253 ha). This change did not explain as much of the changes in Lalan as it did in Mangrove and Kerinci, however, where 6% of overall change could be attributed to regeneration.

Overall, Lalan experienced at least four and one-half times more change than any other study area. In terms of hectares affected, Lalan also showed more change than all the other regions combined. Inversely, Bentayan varied the least between the two study periods, changing only 1,993 hectares of its land cover.

Table 18: Change processes for all project areas in the investigated time period (2014 – 2016).

Process	Benakat	Bentayan	Dangku	Kerinci	Lakitan	Lalan	Mangrove	Reki	Sembilang
Deforestation	456 *12.8%*	1,168 *58.6%*	748 *29.9%*	2,395 *52.7%*	3,683 *64.1%*	53,065 *86.1%*	5,319 *41.7%*	3,709 *46.8%*	21,214 *86.6%*
Forest degradation	2 *0.0%*	92 *4.6%*	1,645 *65.7%*	118 *2.6%*	629 *10.9%*	2,236 *3.6%*	0 *0.0%*	3,895 *49.2%*	366 *1.5%*
Agricultural expansion on non-forest	965 *27.0%*	552 *27.7%*	34 *1.4%*	1,509 *33.2%*	131 *2.3%*	458 *0.7%*	5,594 *43.9%*	44 *0.6%*	642 *2.6%*
Plantation expansion on non-forest	1,902 *53.3%*	140 *7.0%*	46 *1.8%*	123 *2.7%*	1,200 *20.9%*	2,757 *4.5%*	947 *7.4%*	136 *1.7%*	468 *1.9%*
Settlement expansion	8 *0.2%*	0 *0.0%*	0 *0.0%*	2 *0.1%*	0 *0.0%*	0 *0.0%*	44 *0.3%*	0 *0.0%*	22 *0.1%*
Flooding	0 *0.0%*	5 *0.3%*	6 *0.2%*	13 *0.3%*	10 *0.2%*	55 *0.1%*	38 *0.3%*	5 *0.1%*	280 *1.1%*
Land clearing	221 *6.2%*	1 *0.0%*	6 *0.3%*	112 *2.5%*	31 *0.5%*	790 *1.3%*	262 *2.1%*	84 *1.1%*	622 *2.5%*
Regeneration	16 *0.5%*	35 *1.8%*	19 *0.7%*	274 *6.0%*	64 *1.1%*	2,253 *3.7%*	550 *4.3%*	48 *0.6%*	889 *3.6%*
Total change	**3,569**	**1,993**	**2,505**	**4,546**	**5,749**	**61,614**	**12,754**	**7,920**	**24,503**
No change	**48,881**	**64,227**	**32,047**	**234,206**	**75,126**	**38,182**	**79,731**	**62,665**	**209,418**
No Data	**9,063**	**7,626**	**7,703**	**19,547**	**7,168**	**2,061**	**6,906**	**3,567**	**46,821**
Total area	**61,513**	**73,846**	**42,255**	**258,299**	**88,043**	**101,857**	**99,392**	**74,152**	**280,742**

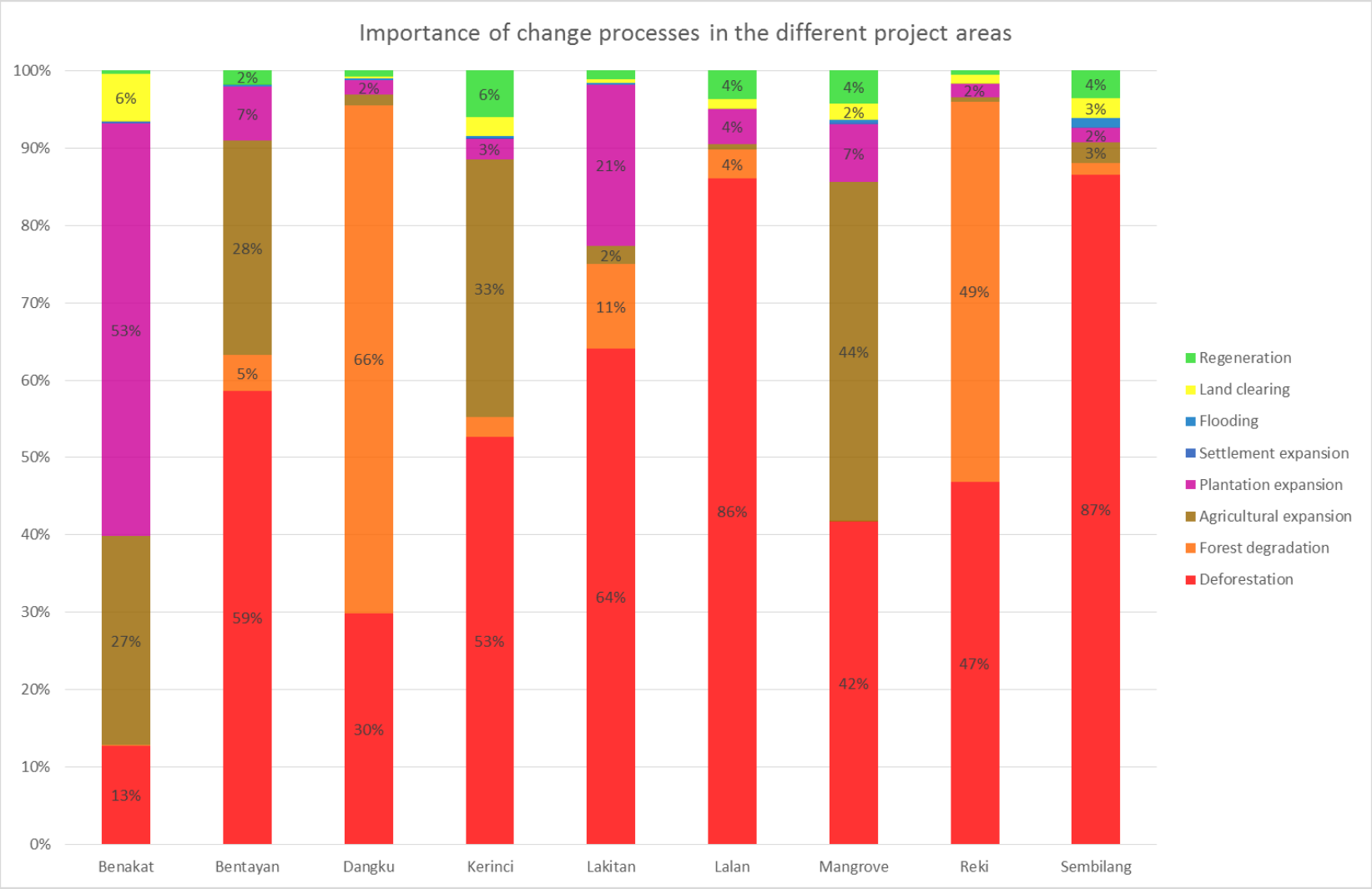

Figure 24: Visual representation of the changes for all project areas in percent (2014 – 2016).

4.3.5. Deforestation rate

Table 19 describes the spatial extent of forest, the net forest loss in hectares and the deforestation rate in percent by project area. The reader is reminded that the following changes were only considered if the area of concern contained data for both time steps.

Table 19: Deforestation rates and net forest loss by study area.

Year	Area Forest [ha]		Net forest loss (ha)	Deforestation rate (%)
	2014	2016		
KPHP Benakat	5,162	4,698	-464	4.5
KPHK Bentayan	11,105	9,909	-1,196	5.4
Dangku WR	25,323	24,565	-759	1.5
Kerinci Seblat NP	152,421	150,001	-2,420	0.8
KPHP Lakitan	17,826	14,109	-3,717	10.4
KPHP Lalan	73,258	20,081	-53,176	36.3
Mangrove	13,655	11,718	-1,936	7.1
PT Reki	62,488	58,755	-3,732	3.0
Sembilang NP	143,741	122,497	-21,244	7.4

According to Table 19, the highest rates of deforestation were observed in KPHP Lalan (36.3%) and KPHP Lakitan (10.4%). These far outweigh the lower rates of deforestation seen in Kerinci Seblat National Park (0.8%) or Dangku Wildlife Reserve (1.5%). A visual representation of these statistics can also be found in Figure 25. Despite its relatively low deforestation rate, Sembilang National Park lost the second largest amount of forest by area (21,244 ha). This quantity was trumped only by the loss in KPHP Lalan, where 53,176 hectares disappeared between 2014 and 2016. KPHP Benakat and Dangku Wildlife Reserve saw the lowest net loss in forest, converting 464 and 759 hectares respectively to other land cover classes (Table 19).

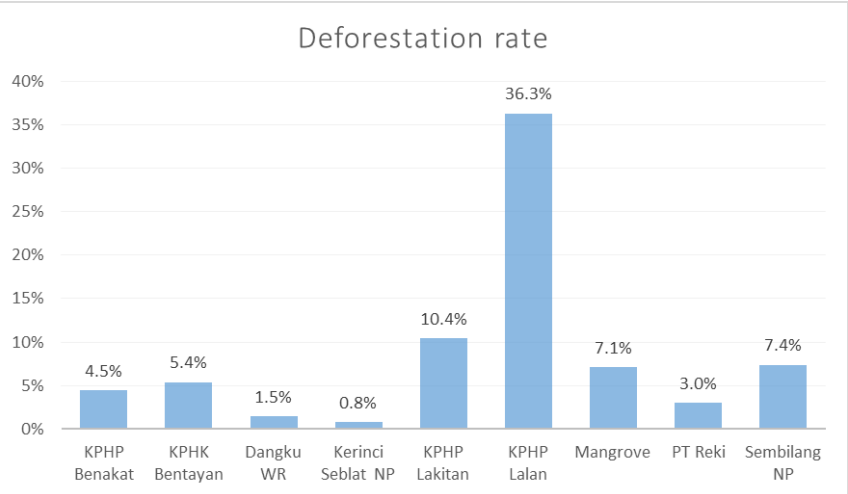

Figure 25: Deforestation rate per project area.

4.3.6. Carbon stock

To derive the carbon stock maps, the local aboveground biomass values derived in Work Package 3 (WP 3) were attributed to the different land cover classes. Carbon stock is reported in tons of carbon (t C). To calculate the carbon content of a certain stratum, the aboveground biomass value is simply divided by 2 (i.e. a carbon content of 0.5 is assumed). By multiplying the extent of the land cover by the carbon content per hectare per land cover class the total carbon stock of the respective land cover class is calculated (stratify & multiply approach).

Table 20 and Figure 26 to Figure 27 exemplarily show the carbon stock results for the Kerinci Seblat National Park project site. The reader is reminded that, in order to make the calculations comparable, a common No Data mask was applied, i.e. only areas which are cloud free and covered with data in Time Steps 1 and 2 are considered in the assessment. A detailed description of all land cover results for all nine project areas can be found in the final report for Work Package 2 (WP 2).

Table 20: Carbon stock of the land cover classes for the years 2014 and 2016 for Kerinci Seblat national Park project site.

Class name	2014	2016
	Carbon (t)	Carbon (t)
High-density lowland dipterocarp forest	11,684,274	11,633,504
High-density lower montane rain forest	5,903,078	5,899,388
High-density upper montane rain forest	305,976	306,128
Medium-density lowland dipterocarp forest	9,200,171	9,034,574
Low-density lowland dipterocarp forest	1,010,160	946,537
Medium-density lower montane rain forest	1,290,816	1,283,769
Low-density lower montane rain forest	83,214	82,544
Low-density upper montane rain forest	193,248	193,344
Dryland agriculture mixed with shrub	26,358	133,297
Oil palm plantation	40	1,112
Rubber Agroforestry	3,893,027	3,739,517
Scrubland	203,238	197,775
Dryland agriculture	98,937	29,419
Bare area	-	-
Settlement	-	-
Road	-	-
Water	-	-
Wetland	54	54
	33,892,589	**33,480,960**

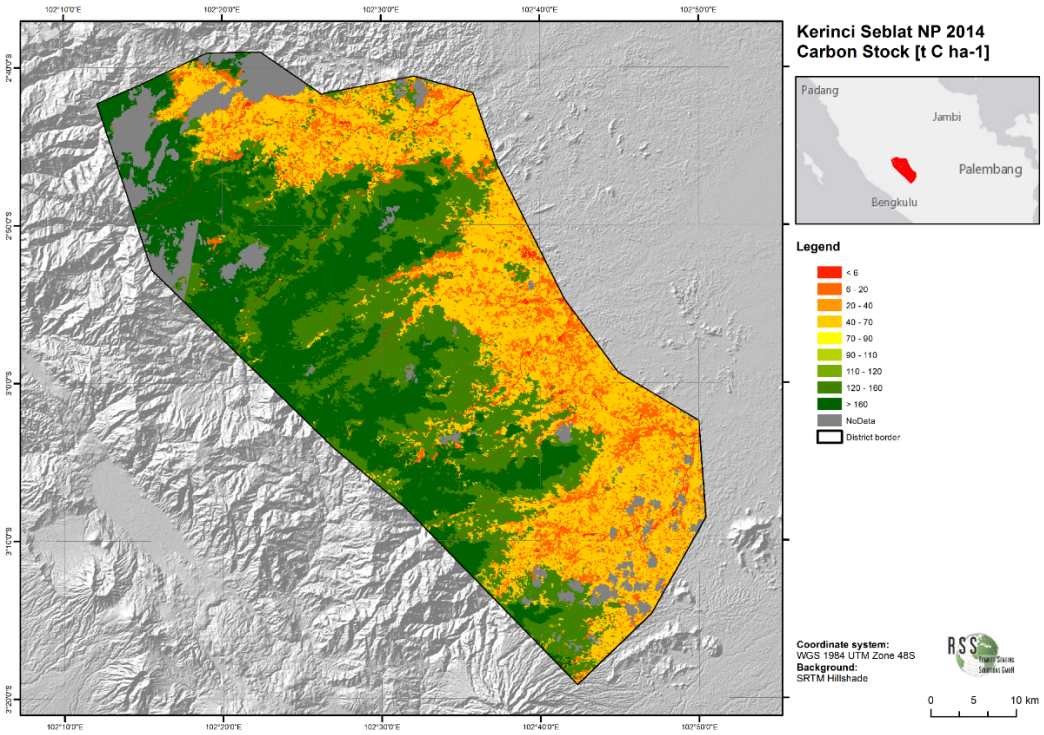

Figure 26: Carbon stock map for the Kerinci Seblat National Park project site (2014).

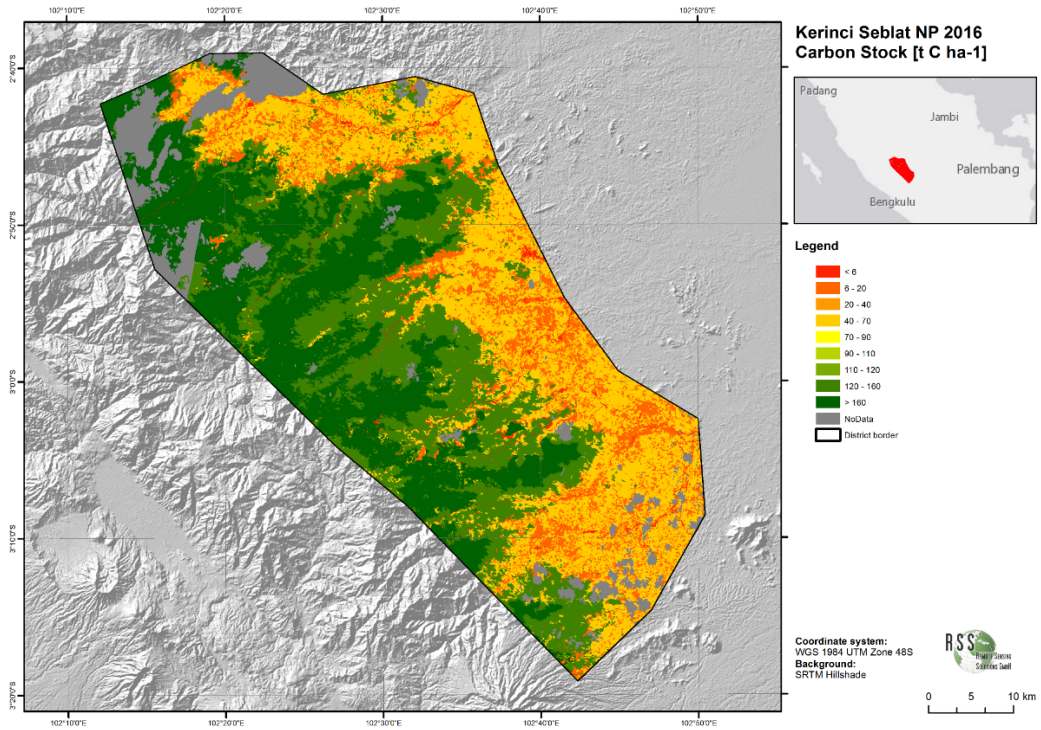

Figure 27: Carbon stock map for the Kerinci Seblat National Park project site (2016).

4.3.7. Carbon stock change

The carbon emission estimates were conducted based on a stock difference approach. This approach specifically assesses the carbon stock stored in different land cover classes between time steps 1 and 2. Here also common Na Data areas were considered. A detailed description of the carb stock changes for the nine project sites can be found in the final report of Work Package 2.

Carbon fluxes were also assessed by studying the average carbon stock per hectare in each study area and for both time steps (Figure 28). This measure directly compares the carbon stocks found in each of the nine study areas.

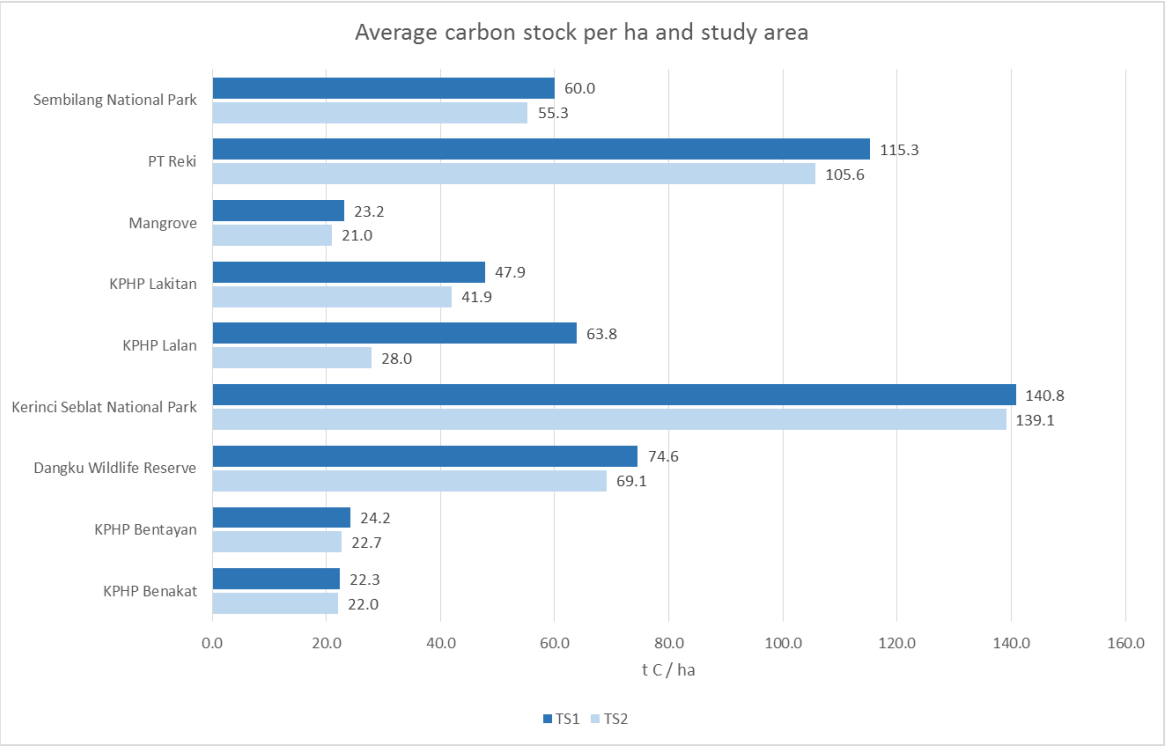

Figure 28: Average carbon stock per hectare and study area.

With 140.8 tons of carbon per hectare in 2014 and 139.1 tons of carbon in 2016, Kerinci Seblat National Park stores the highest average carbon stock of all project areas. Kerinci also experienced the lowest change in average carbon stock (1%) during this period (Figure 28).

The second highest average carbon stock is stored in PT Reki (115.3 t C in time step 1 and 105.6 t C in time step 2). Reki also lost 8% of its average carbon stock per hectare due to forest fires between 2014 and 2016.

Large expanses of industrial forest and acacia plantation push KPHP Benakat's average carbon stock down, making it the region with the lowest amount of carbon per hectare (22.3 t/ha for time step 1 and 22.0 t/ha in time step 2). Furthermore, land cover conversion in this region progressed to such a degree, that KPHP Benakat's reduction in average carbon stock was also notably low (2%).

The highest reduction in average carbon stock took place in KPHP Lalan. Extensive forest fires in the region reduced KPHP Lalan's average carbon stock by 56%, from 63.8 t/ha in time step 1 to 28.0 t/ha in time step 2 (Figure 29).

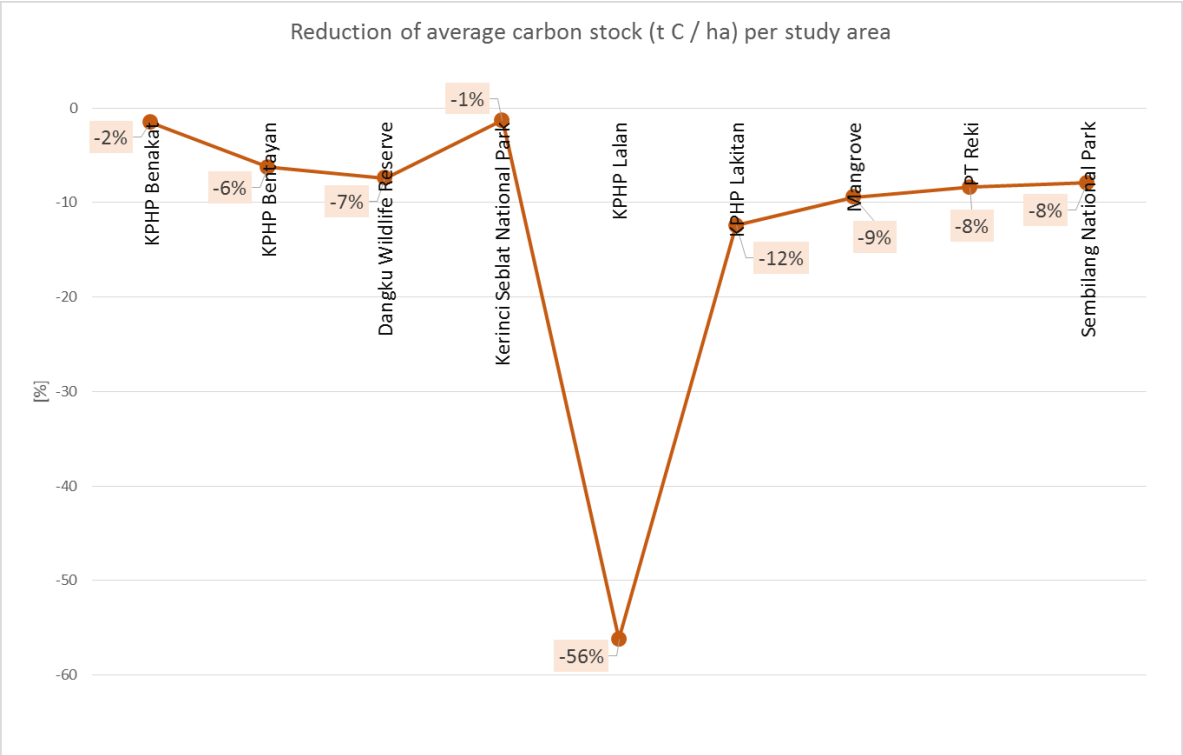

Figure 29: Reduction of average carbon stock per study site in percent.

4.4. Work Package 4: Historic fire regime

Figure 30 shows the flowchart of the activities carried out in Work Package 4 (WP 4): Historic fire regime. The approach chosen to assess the historic fire regime is transferrable to other optical satellite sensors (besides Landsat).

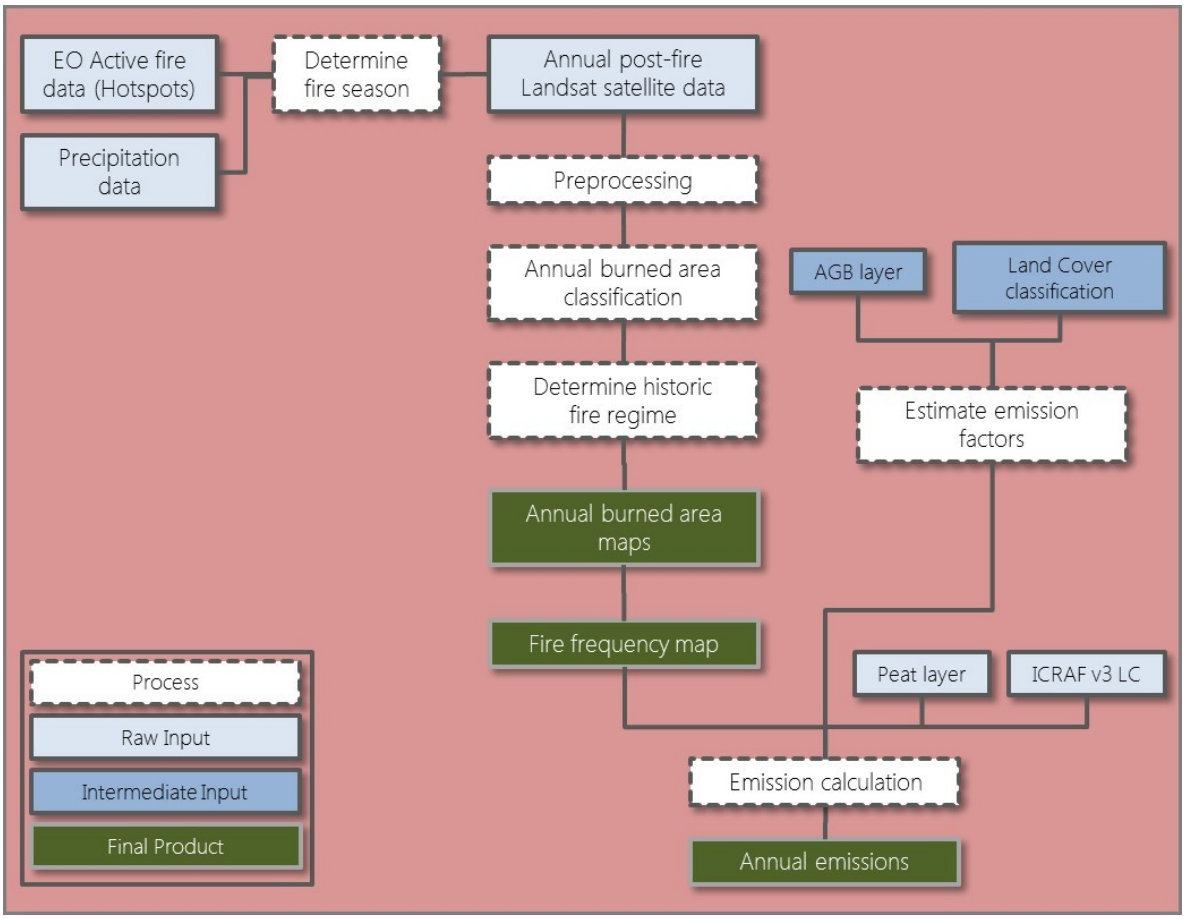

Figure 30: Flow chart of the activities carried out in Work Package 4 (WP 4): Historic fire regime.

4.4.1. Selection of annual mid resolution images for the years 1990 – 2014

In a first step, the fire season of each year was analyzed on the basis of monthly precipitation and MODIS active fire hotspot data. The latest MODIS Collection 6 hotspot data was provided by the University of Maryland's Fire Information for Resource Management System (FIRMS) as point shapefiles for the time period 2000 onwards. The fire season of the pre-MODIS era (before the year 2000) was investigated based on active fire data from the Forest Fire Prevention and Control Project of the European Union and the South Sumatra Forest Fire Management Project (SSFFMP). In addition, the Oceanic Niño Index (available at: http://www.cpc.ncep.noaa.gov/products/analysis_monitoring/ensostuff/ensoyears.shtml), indicating El Niño years with higher fire occurrence, was additionally implemented as indicator for fire seasons with high fire probability.

Available mid-resolution multispectral imagery was selected from fire season start to approximately two months after fire season end. Landsat-5, Landsat-7 or Landsat-8 images were used for the assessment of the annual burned area. Figure 31 displays the number of MODIS hotspots within the BIOCLIME project area, the years selected for burn area mapping and the number of Landsat scenes considered for the mapping years.

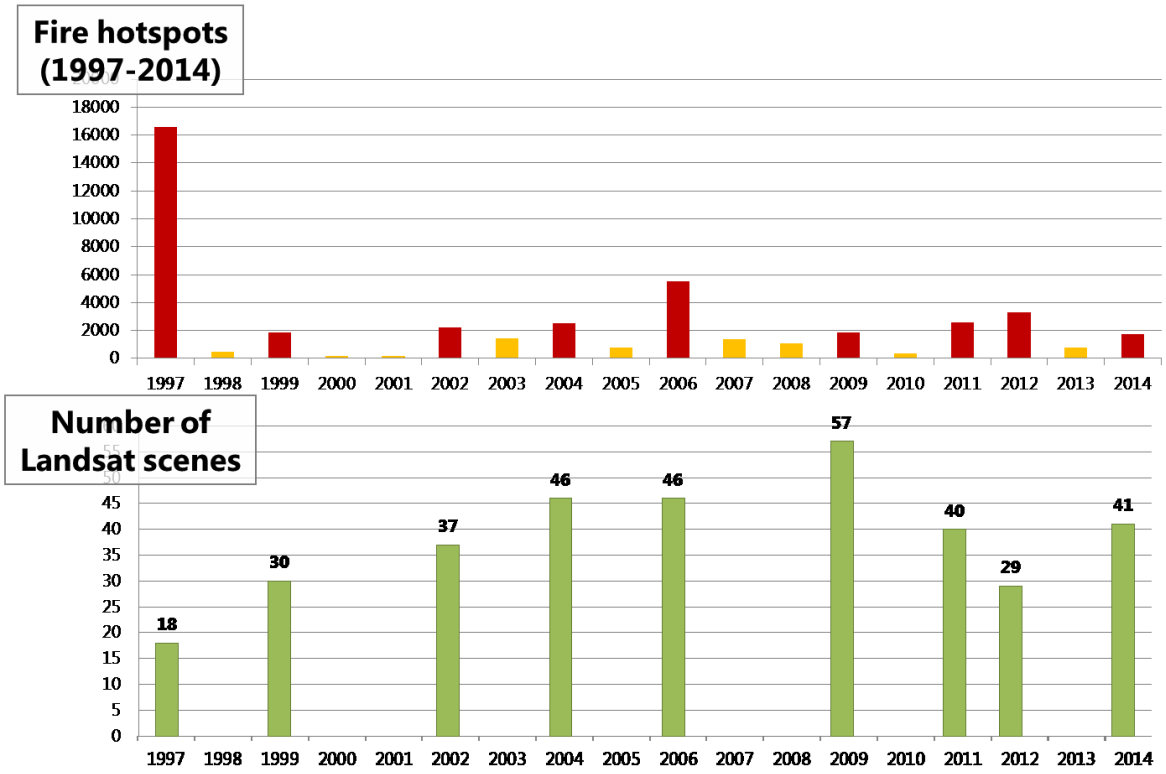

Figure 31: The upper diagram shows the number of MODIS hotspots within the BIOCLIME project area from 1997 to 2014. Red bars indicate the years selected for mapping, yellow bars indicate the years not mapped. The lower diagram depicts the number of considered Landsat scenes for the years mapped.

4.4.2. Preprocessing

The pre-processing for Landsat data consisted of the removal of atmospheric distortions (scattering, illumination effects, adjacency effects), induced by water vapor and aerosols in the atmosphere, seasonally different illumination angles, etc. An atmospheric correction was applied to each image using the software ATCOR (Richter and Schläpfer 2014).

4.4.3. Burned area

Annual burned areas were classified based on different burned ratios and the normalized difference vegetation index (NDVI). A combination of two object-based classification approaches (approach one: single scene; approach two: multiple scene change detection) was implemented to overcome particular limitations of each single approach. Combining both outputs lead to the best results of burned area classification. After the automatic classification manual revision was necessary especially in areas with a lot of smoke and/or haze. Figure 32 graphically depicts the two approaches and their combination.

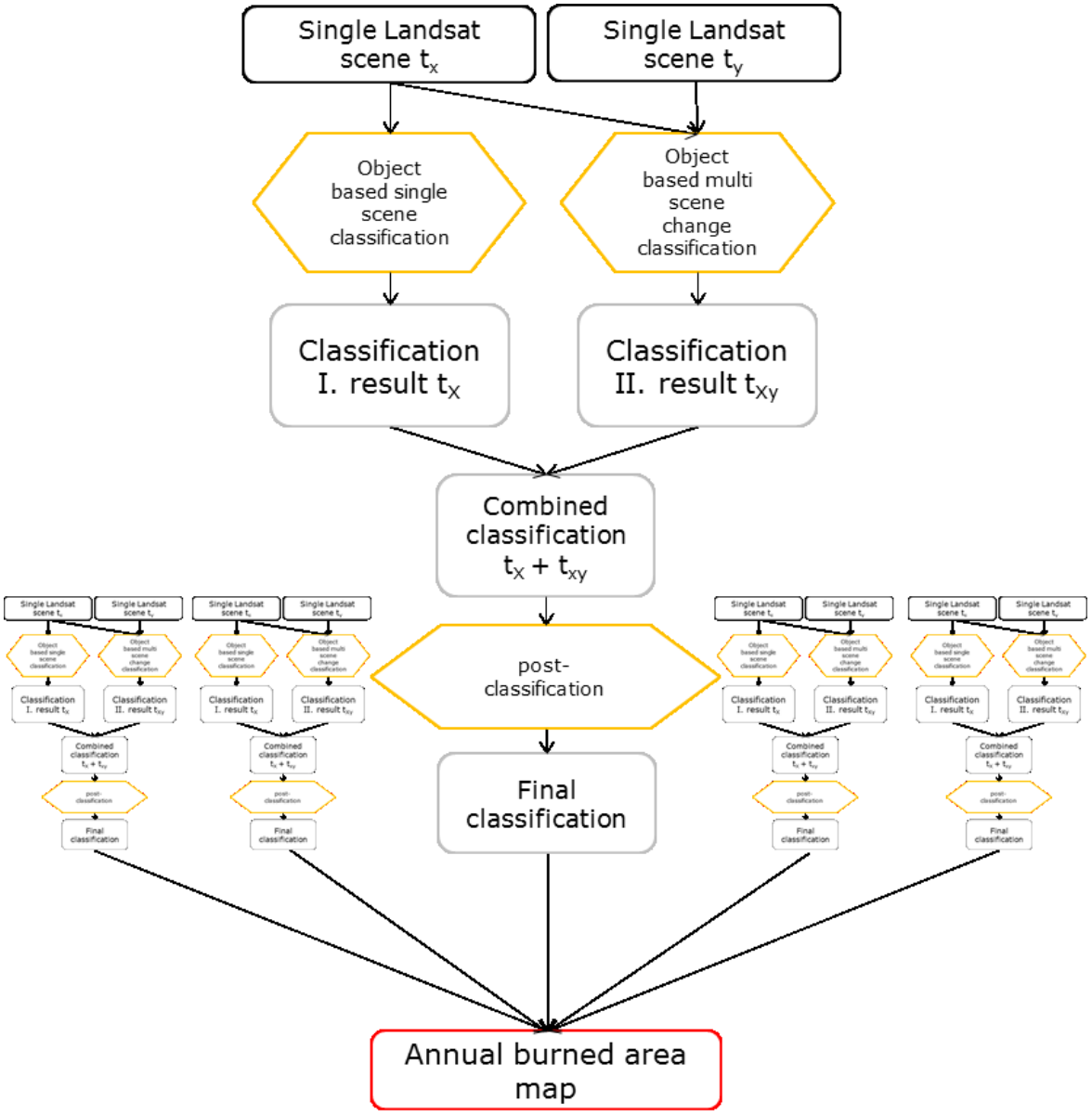

Figure 32: This figure represents both burned are classification workflows and their fusion.

Burned area maps for 9 different years (1997, 1999, 2002, 2004, 2006, 2009, 2011, 2012 and 2014) were generated. In addition, a burned area map for 2015 based on Sentinel-1 RADAR data was provided from the ESA (European Space Agency) funded Fire CCI (Climate Change Initiative) project, and was integrated into the analysis and results (see Figure 33).

Based on these maps a fire frequency map (a compilation of the single year classifications) was derived (see Figure 34).

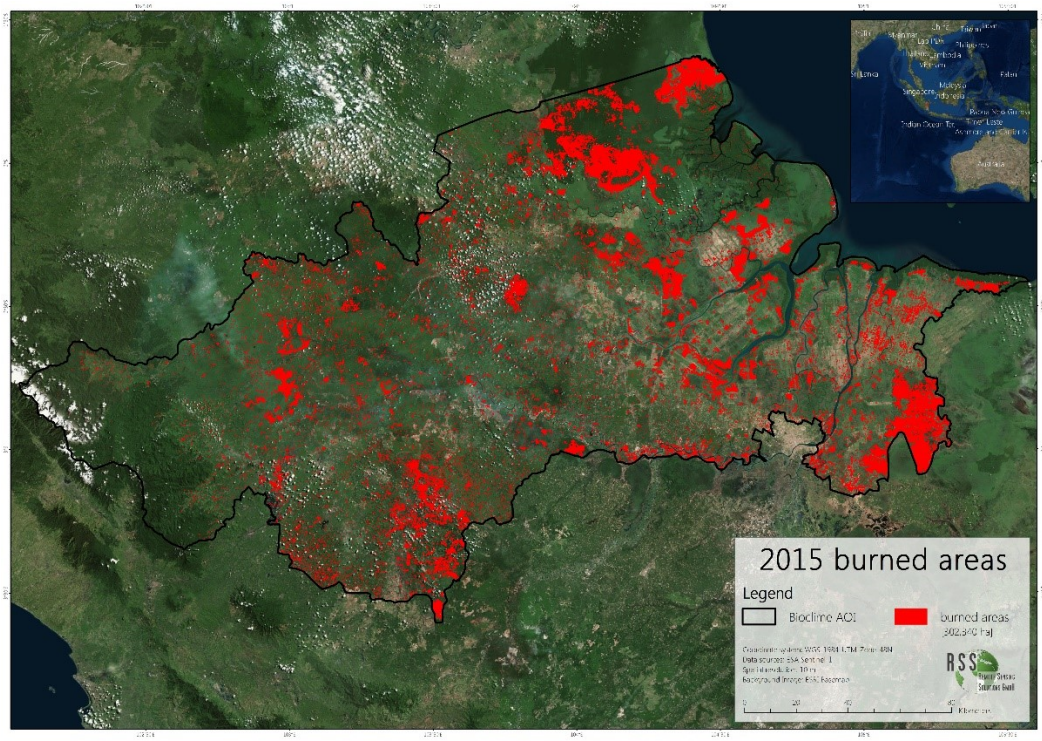

Figure 33: Burned area map for the year 2015 based on Sentinel-1 data (CCI Fire Project).

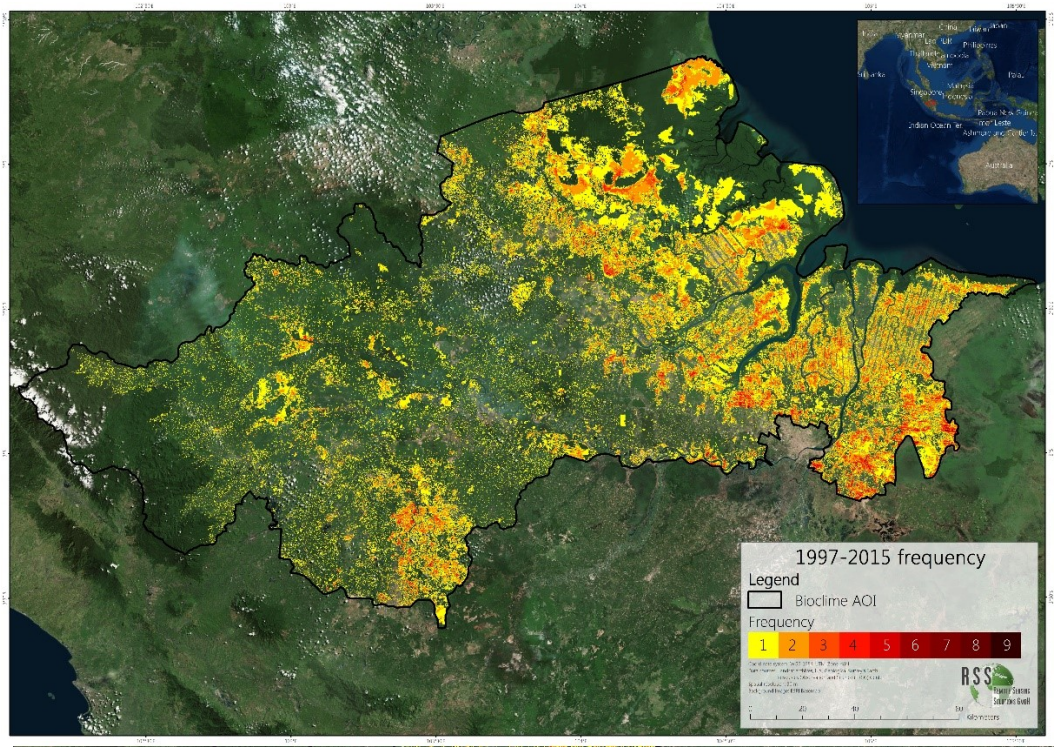

Figure 34: Fire frequency map combining the burned areas of the years 1997, 1999, 2002, 2004, 2006, 2009, 2011, 2012, 2014 and 2015.

Table 21 shows the number of satellite scenes used, the amount of hotspots detected and the total area burned for each year. For the years 1997 (333,931 ha) and 2015 (323,397 ha), by far, the most area burned was detected, with 1997 even higher than 2015.

Table 21: Statistical information about the classified years. Shown are the number of satellite scenes used, the amount of hotspots detected and the total area burned for each year.

Year	No. Scenes	Hotspots	Total Area Burned [ha]
1997	18	16,573	333,931
1999	30	1,888	64,009
2002	37	2,216	119,204
2004	46	2,515	120,029
2006	46	5,494	243,560
2009	57	1,875	68,172
2011	40	2,592	89,310
2012	29	3,319	164,246
2014	41	1,755	53,440
2015	Sentinel-1	8,582	323,397

Figure 35 displays a comparison between the yearly burned area classified and the amount of hotspots detected for the respective years. From this figures it is visible that there is a general trend, but no definite correlation between the amount of hotspots detected and the area burned, so that a direct deduction of burned area from hotspots should always be treated with caution (see also Table 21).

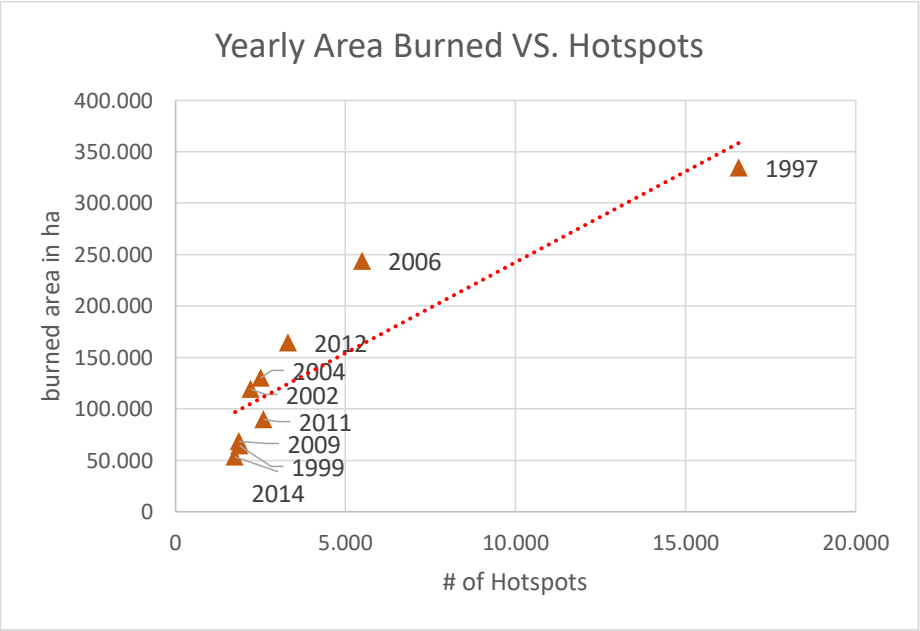

Figure 35: Graph depicting the number of MODIS Hotspots detected during the selected years within the BIOCLIME study area and the mapped burned area for each year in hectares.

4.4.4. Pre-fire vegetation

Further, the land cover classification produced by ICRAF for the years 1990, 2000, 2005, 2010 and 2014 (see Work Package 1 (WP 1): Historic land cover change and carbon emission baseline) was used in order to assess pre-fire land cover class. This helps the identification of the drivers of deforestation. Furthermore, this allows an estimation of the carbon emissions released by fire in South Sumatra since 1990. Figure 36 depicts the area burned per land cover class for each year. In 1997 the share of burned primary forest is by far the biggest compared to the other years. 165,865 ha of "Primary swamp forest", 17,710 ha of "Primary dry land forest" and also 3,282 ha of "Primary mangrove forest" burned in 1997. In total this sums up to 186,857 ha of burned primary forest in 1997. The second largest primary forest burning in the BIOCLIME project area took place in 2006 with only (compared to 1997) 17,133 ha of burned primary forest in total. The burning of the land cover class "Tree crop plantation" is increasing over the years and in 2015 more than 106,773 ha of it burned. The same increase over time is visible for the class "plantation forest" where more than 29,275 ha burned in 2015. There is a clear change in ratio of land cover classes burned over the last two decades.

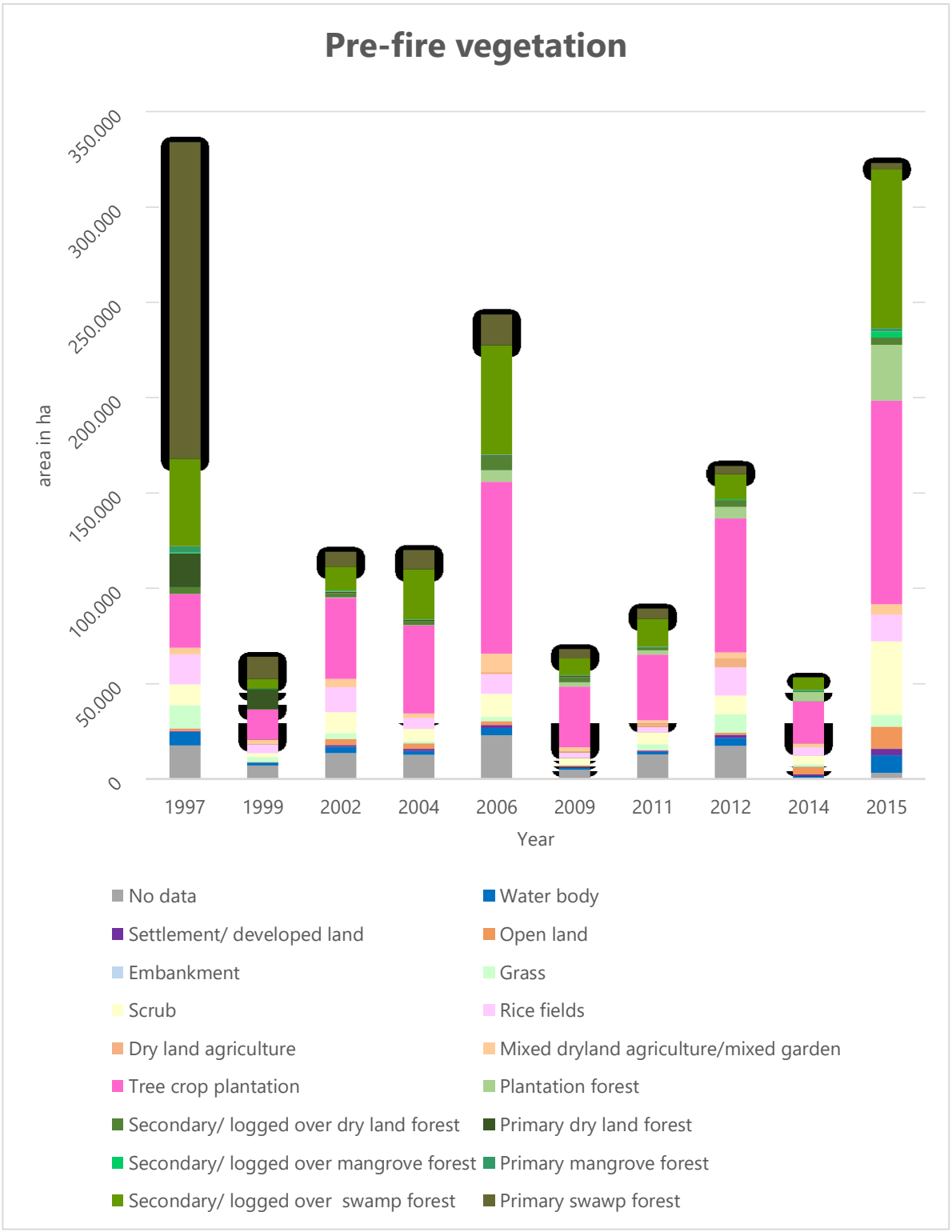

Figure 36: This graph depicts which land cover has burned to which extend within the different years.

4.4.5. Emissions

To calculate the emissions by the fires for each year, the aboveground emissions and peat emissions were calculated. Summing these products up leads to total emissions for each single mapped year.

We used the stratify & multiply approach to calculate carbon stock maps from the land cover classifications of Work Package 1 (WP 1) in combination with the local aboveground biomass values derived in Work Package 3 (WP 3), and intersected those carbon stock maps with the fire frequency map for the calculation of the emissions. Emissions are reported in tons of carbon (t C). To calculate the carbon content of a certain stratum, the biomass is simply divided by 2 (i.e. a carbon content of 0.5 is assumed). By multiplying the burned area with the carbon stock the carbon emissions from burning biomass are calculated.

In addition, the carbon emissions from peat burning were calculated. To calculate these emissions, we used the approach by Konecny *et al.* (2016), which discriminates between first, second and or more fires with regard to the peat burn depth, and therefore the amount of carbon which is released. To generate the peat emissions, the land cover, burned area and peat layers (Peatland distribution for 2016 created by Ministry of Environment and Forestry (MoEF) were intersected. Similar to the emission estimation from aboveground biomass, the pre-fire land cover is taken into consideration. Burned areas within formerly forested peatlands are considered to be first-fires and therefore a burn depth of 17 cm is applied (see Konecny *et al.* 2016). All other land cover classes are then assigned to second or more fires with a reduced burn depth. So only two different stages of fires (first and second or more) were discriminated.

Table 22 depicts the aboveground carbon emissions for each mapped year, as well as the peat emissions and the total emissions in megatons of carbon (Mt C). The highest emissions were calculated for 1997 with 46.71 Mt C followed by 2015 with 21.42 Mt C, 2006 with 16.07 Mt C and 2012 with 8.05 Mt C. Further it is visible that emissions are not directly connected to the total burned area. This is also shown in Figure 37, where the X-Axis depicts the years, the Y-Axis the burned area in hectares and the diameter of the circles the amount of carbon emissions. It can be concluded that different land covers lead to different emissions, further the distribution of the peat layer also plays an important role in the amount of emissions.

Table 22: Emissions per year megatons of carbon (Mt C), split up into aboveground (above) and peat emissions.

Year	Area burned (ha)	Emissions (Mt C)		
		Above	Peat	Total
1997	333,931	26.99	20.36	47.35
1999	64,009	3.87	2.01	5.88
2002	119,204	3.02	2.96	5.98
2004	120,029	3.18	3.17	6.35
2006	243,561	7.41	9.45	16.86
2009	68,172	1.84	1.49	3.33
2011	89,310	2.19	3.64	5.83
2012	164,246	2.92	5.70	8.62
2014	53,440	1.03	1.67	2.70
2015	323,397	7.15	14.26	21.42
Total	**1,579,297**	**59.60**	**64.71**	**124.31**

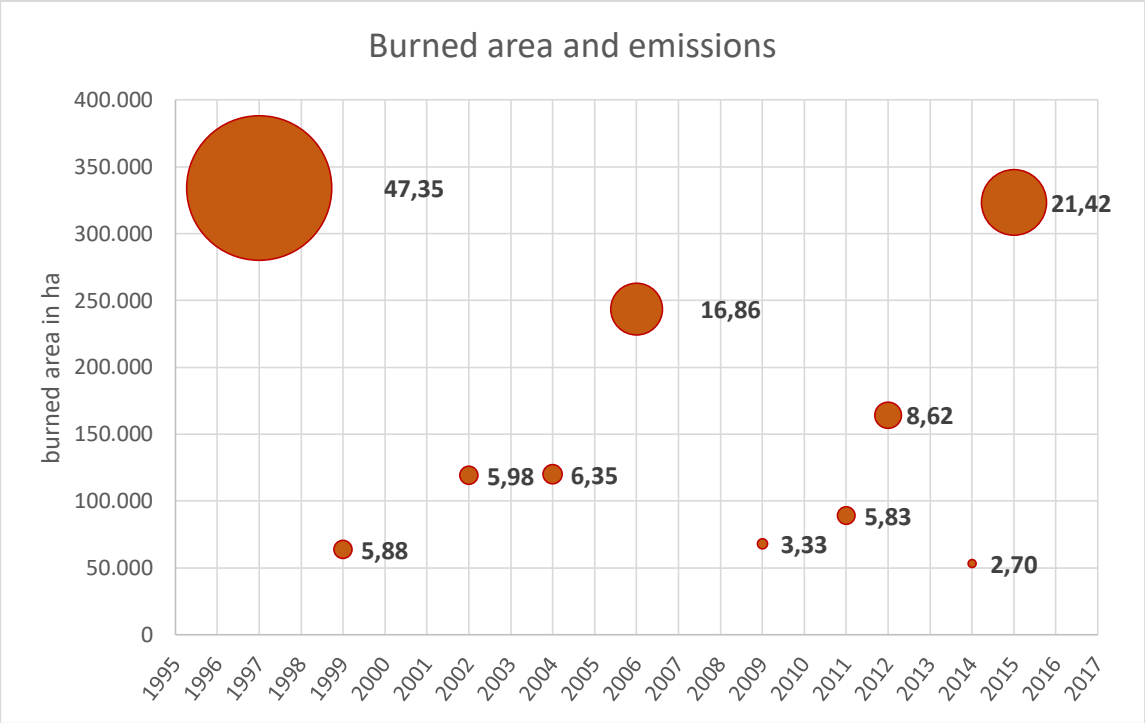

Figure 37: The burned area in ha (Y-axis) for each mapped year (X-axis). The diameter of each circle depicts the emissions in megatons of carbon (Mt C).

Figure 38 Displays the total emissions divided into aboveground and peat emissions in megatons of carbon (Mt C). this figure shows that the ratio of emissions from aboveground biomass to peat changes over time. In the past proportionally more emissions were from aboveground biomass burning whereas in recent years proportionally more emission from peat burning.

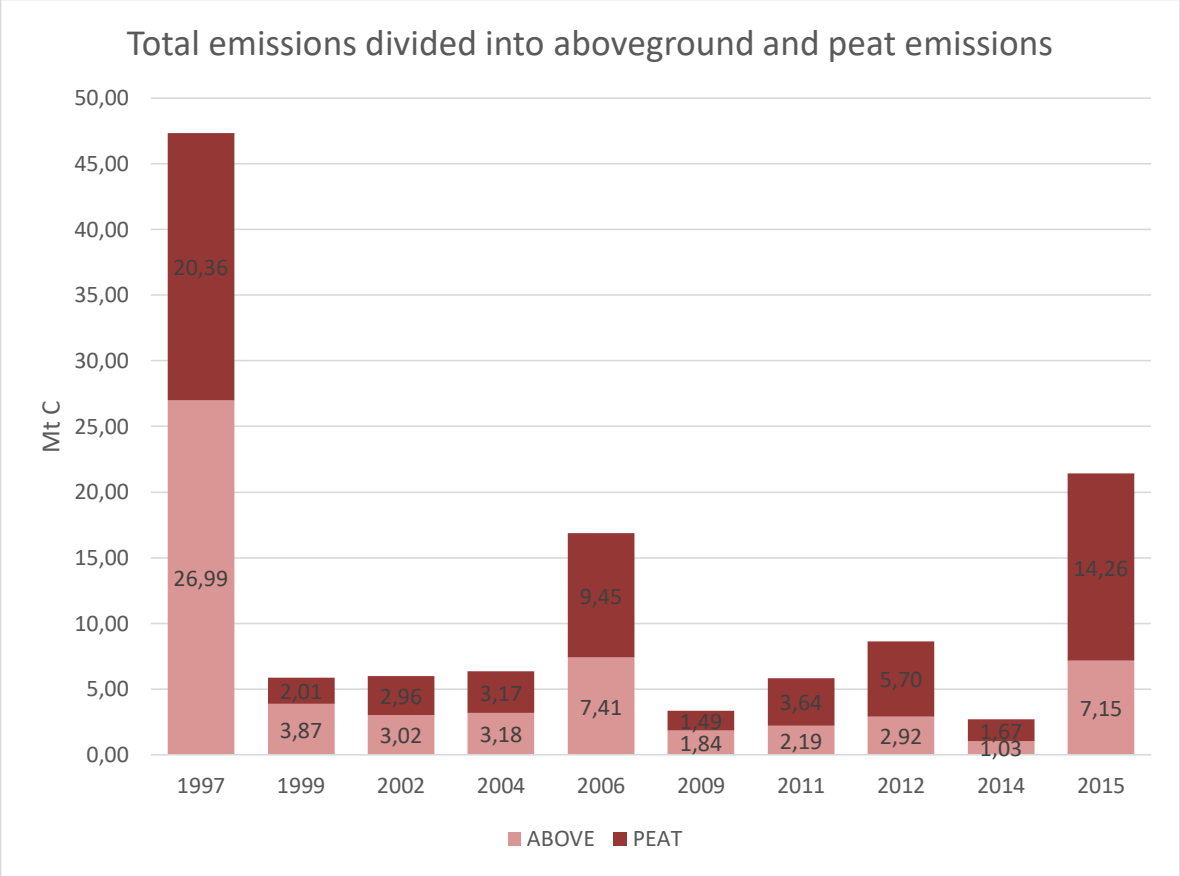

Figure 38: Total emissions divided into aboveground and peat emissions in megatons of carbon (Mt C). The light red bars depict the carbon emissions of the aboveground biomass (ABOVE) and the dark red bars the peat emissions (PEAT).

5. Conclusions and outlook

5.1. Work Package 3 (WP 3): Aboveground biomass and tree community composition

Following conclusions could be drawn (separated into the aboveground biomass and the tree community composition modelling).

Aboveground biomass modelling

- Local aboveground biomass (AGB) values could be derived from the LiDAR based aboveground biomass model for almost all identified vegetation cover classes.
- High aboveground biomass variability within vegetation classes could be identified (e.g. Primary Dryland Forest has a standard deviation for aboveground biomass of ±165.5 t/ha).
- Areas with the highest aboveground biomass (AGB) values were located within and around the Kerinci Seblat National Park.

Tree community composition modelling

- The findings of this study indicate that the similarity in tree community composition can be predicted and monitored by means of airborne LiDAR.
- In addition to using airborne LiDAR data as mapping tool for aboveground biomass this data could be further developed to provide a biodiversity mapping tool, so that biodiversity assessments could be carried out simultaneously with aboveground biomass analyses (same dataset).
- A further advantage of the approach is that the tree community composition can be carried out without identifying individual tree crowns in remotely sensed imagery.

A next step would be to harmonize the results from the carbon plots. As the aboveground biomass calculations derived by the experts from the Bogor Agricultural University (IPB) are based on more differentiated allometric equations (e.g. species specific) it is recommended to use these aboveground biomass estimates to calibrate the LiDAR based aboveground biomass model, which would lead to revised local aboveground biomass values for the different vegetation classes. This consequently would lead to a recalculation of the emissions derived in Work Packages 1, 2 and 4.

Further interesting research topics would be:

- It would be of interest to analyse the abundance of pioneer and climax species within the different biodiversity plots.
- Also of interest would be a spatial comparison of the LiDAR based aboveground biomass model with the LiDAR based tree community composition model.
- Finally, it would also be interesting to analyse what influence do different historical land use patterns (e.g. logging) have on the aboveground biomass and tree community composition for similar forest classes (e.g. Secondary Dryland Forest), that were classified on the basis of multispectral satellite imagery.

5.2. Work Package 1 (WP 1): Historic land cover change and carbon emission baseline

Following conclusions could be drawn:

- The BIOCLIME study area is dominated by Tree crop plantations which constantly increased in spatial extent over the whole observation period by over 600,000 ha, culminating at 1,461,231 ha in 2014.
- All forest types lost in spatial extent over the observation period, the most intense forest losses in absolute terms were found in Primary swamp forest (-578,818 ha) and Primary dryland forest (-364,692 ha). While the former was almost disappeared in 2014 (only 47,206 ha of former 626,024 ha left), the latter has retained 171,254 ha or 32 % of the original 535,947 ha. While significant parts of these losses were in the first observation window 1990 – 2000 due to logging and consequent conversion to secondary forest, deforestation clearly dominated over time as a driver of primary forest loss.
- Land cover categories which increased in size include, aside from tree crop plantation, Plantation forest (+107,682 ha), Shrub (+64,357 ha), Open land (+52,928 ha), Settlement (+37,391 ha) and Mixed dryland agriculture/ mixed garden).
- The analysis of change drivers revealed that Deforestation accounts for 63% of all changes observed between 1990 and 2014, followed by forest degradation with 20% and Plantation expansion on Non-forest with 12%.

- Net forest loss amounted to 55% or 865,286 ha in total over the whole observation period. Annual deforestation rates increased from 2.3% yr-1 between 1990 and 2000 to 3.8% yr-1 between 2005 and 2010 and then further to 4.9% yr-1 between 2010 and 2014. This increase is due to varying but more or less constant net forest loss compared to ever decreasing forested areas.
- The main driver of deforestation was found to be conversion to tree crop plantation accounting for 65% of all deforestation. However, when observed through time, this driver lost importance since the period 2000 – 2005 with 74% of all deforestations down to 43%. This shows a trend in tree crop plantation development to move away from forested areas to the development of already deforested areas. Other important drivers of deforestation were "Conversion to shrub" and "Conversion to Plantation forest" accounting for approximately 10% of all deforestation in the overall observation period.
- The analysis of carbon stock distribution over time shows the highest carbon storage was and is found in Primary dryland forest with 46,666,832 t C in 2014. However, the second highest carbon stocks are found in the Tree crop plantation class which accounts for 23,379,703 t C in 2014 due to its dominant spatial extent in the study area. Secondary dryland forest with 17,472,038 t C has the next highest carbon stocks followed by Primary mangrove forest with 12,724,300 t C.
- The most intensive carbon losses were observed in the class Primary dryland forest, amounting to -99,378,611 t C followed by Primary swamp forest with 65,406,453 t C. These intense losses were only partly compensated by carbon accumulation in Tree crop plantations amounting to 9,811,331 t C and Plantation forest (2,153,637 t C).
- Annual total carbon losses amounted totaled at -8,767,278 t C yr-1 in the period 1990-2000, constantly declining to -4,410,966 t C yr-1 in the period 2010 – 2014. The overall average 1990 – 2014 was -6,032,284 t C yr-1
- The analysis of the drivers of carbon emissions showed that the main process causing emissions is the conversion into tree crop plantations which account for almost 80,000,000 t C in the observation period 1990 – 2014. The majority of those emissions came from the conversion of Primary dryland forest, followed by Primary swamp forest. The second highest emissions were caused from logging of Primary dryland forest, accounting for approximately 16,000,000 t C followed by the conversion to Plantation forest which produced another 13,000,000 t C. Logging of primary swamp forest caused another 11,000,000 t C.
- A simple carbon emission baseline was drawn for the study area based on the historic development of total carbon stock and a trend analysis. The historic trend follows a logarithmic decline, which was projected forward until the year 2040. The projected carbon stock in the year 2040 amounts to approximately 75,000,000 t C which means the predicted emissions under a business as usual scenario amount to approximately 50,000,000 t C in the next 25 years, i.e. approximately 2,000,000 t C yr-1 as a long term annual average.

5.3. Work Package 2 (WP 2): Forest benchmark mapping and monitoring were:

Following conclusions could be drawn:

- Although the land cover classification scheme developed was based on the BAPLAN classification scheme, the scheme presented included more detailed forest and degradation

classes. The details added can be easily reverted to the broader, official classification scheme if necessary.

- The benchmark land cover maps produced have a high overall thematic accuracy (84.4% according to the BAPLAN classification scheme) which makes them an ideal basis for future monitoring.
- Kerinci Seblat National Park is the only region where RapidEye coverage was incomplete and a filling with Landsat-8 imagery was required.
- The way the classification algorithm was designed allowed it to be easily transferred and applied to the images from the second time step and also enabled the maps from the second time step to achieve an overall accuracy of 87%.
- The lowest percentwise decrease in carbon stock per hectare was found in Kerinci Seblat National Park (1%) and KPHP Benakat (2%). Medium-density lowland dipterocarp forest in Kerinci Seblat National Park lost the most carbon (165,597 t C), experiencing a deforestation rate of just 0.8%. Meanwhile, KPHP Benakat experienced a relatively high deforestation rate of 4.5% proportional to its decrease in carbon stock. In Benakat, loss of low-density lowland dipterocarp forest had the largest impact, removing 28,004 tons of carbon.
- In KPHP Bentayan reduced carbon stock per hectare was reduced by around 6%, documenting a deforestation rate of 5.4%. Furthermore, although carbon losses in non-forest classes were greater than those in forest classes, net forest loss still amounted to 1,196 ha in KPHP Bentayan.
- In the Dangku Wildlife Reserve a immense carbon stock loss was observed within medium-density lowland dipterocarp forests (267,793 t C). This led to a 7% reduction in average carbon stock per hectare, a net forest loss of 759 hectares and finally, a deforestation rate of 1.5%.
- PT Reki and Sembilang National Park both experienced an 8% loss in average carbon stock per hectare. However, the percent deforestation rate in Sembilang National Park (7.4%, 21,244 ha) was more than twice the amount (3%, 3,732 ha) lost in PT Reki.
- With a 9% reduction in average carbon stock per hectare, Mangrove lost the majority of its carbon (133,804 t C) through the nipah palm class. This equated to a net forest loss of approximately 1,936 ha and resulted in a deforestation rate of 7.1%.
- The second largest reduction in average carbon stock amounted to 12% and was found in KPHP Lakitan. Within Lakitan, medium-density lowland dipterocarp forest lost approximately half a million tons, the net forest loss amounted to 3,717 hectares and a deforestation rate of 10.4% was recorded.
- The highest reduction of average carbon stock was by far was recorded in KPHP Lalan at 56%. In this region, high-density peat swamp forest alone lost more than three million tons of carbon. This contributed to a deforestation rate of 36.3% and a net forest loss of 53,176 ha.

5.4. Work Package 4 (WP 4): Historic fire regime were:

Following conclusions could be drawn (separated into burned area, carbon emissions from fires and ratio between carbon emission from aboveground biomass and peat burning).

Burned area

- A direct deduction of burned area from the amount of fire hotspots should always be treated with caution (only general trend).
- In 1997 the share of burned Primary Forest is by far the biggest.

- The second largest Primary Forest burning took place in 2006.
- The burning of the land cover classes Tree Crop Plantation and Plantation Forest is increasing over the years.
- There is a clear change in ratio of land cover classes burned over the last two decades.

Carbon emission from fires

- The years with the highest carbon emissions (megatons of carbon Mt C) from fire were:
  - 1997 with 46.71 Mt C (megatons of carbon)
  - 2015 with 21.42 Mt C
  - 2006 with 16.07 Mt C
  - 2012 with 8.05 Mt C
- Emissions are not directly connected to the total burned area.
- Different land covers lead to different emissions, further the distribution of the peat layer also plays an important role in the amount of emissions.

Ration between carbon emissions from aboveground biomass and peat burning

- The ration of emissions from aboveground biomass to peat burning changes over time.
- In the past proportionally more emissions from aboveground biomass burning.
- In recent years proportionally more emissions from peat burning.

6. Outputs / deliverables

6.1. Work Package 3 (WP 3): Aboveground biomass and tree community composition

- Processed and filtered LiDAR data (.las format)
- Digital Surface Model (DSM) in 1 m spatial resolution (.img format)
- Digital Terrain Model (DTM) in 1 m spatial resolution (.img format)
- Canopy Height Model (CHM) in 1 m spatial resolution (.img format)
- LiDAR based aboveground biomass model in 5 m spatial resolution (.img format)
- Local aboveground biomass values (tables in final report)
- LiDAR based tree community composition model for Lowland Dipterocarp Forest in 31.25 m spatial resolution (.img format)

6.2. Work Package 1 (WP 1): Historic land cover change and carbon emission baseline

- Land cover classifications 1990, 2000, 2005, 2010, 2014 in the BAPLAN classification scheme, in Shapefile format
- Common No Data mask for the time period 1990 – 2014

- Land cover change, carbon stock, and carbon stock change for the time periods 1990 – 2000, 2000 – 2005, 2005 – 2010 and 2010 – 2014, in Shapefile format
- Land cover change, deforestation and GHG emission statistics, in Excel format

6.3. Work Package 2 (WP 2): Forest benchmark mapping and monitoring were:

- Land cover classification, TS1 and TS2 in Shapefile format
- Carbon stock, TS1 and TS2 in Shapefile format
- Field/validation data, TS1 and TS2 in Shapefile format
- Land cover change in Shapefile format
- Satellite data, RapidEye, Spot and Landsat (Type: tiff, bsq)

6.4. Work Package 4 (WP 4): Historic fire regime were:

- Vector data of fire frequency combining the burned areas of the years 1997, 1999, 2002, 2004, 2006, 2009, 2011, 2012, 2014 and 2015 (.shp format)
- Statistics on burned areas and emissions (tables in final report)
- Final report (.docx format)

References

Asari N., Suratman M.N., Jaafar J., Khalid M.M. (2013). Estimation of Above Ground Biomass for Oil Palm Plantations Using Allometric Equations. 2013 4th International Conference on Biology, Environment and Chemistry, IPCBEE vol. 58, IACSIT Press, Singapore, doi: 10.7763/IPCBEE.2013.V58.22.

Ballhorn U., Jubanski J., Siegert F. (2011). ICESat/GLAS Data as a measurement tool for peatland topography and peat swamp forest biomass in Kalimantan, Indonesia. Remote Sens. 3, 1957–1982.

Barlow J., Gardner T.A., Araujo I.S., Avila-Pires T.C., Bonaldo A.B., Costa J.E. et al. (2007). Quantifying the biodiversity value of tropical primary, secondary, and plantation forests. Proceedings of the National Academy of Sciences of the United States of America, 104, 18555–18560.

Chave J., Réjou-Méchain M., Búrquez A., Chidumayo E., Colgan M.S., Delitti W.B. et al. (2014). Improved allometric models to estimate the aboveground biomass of tropical trees. Global Change Biology, 20(10), 3177-3190.

Chave J., Andalo C., Brown S., Cairns M.A., Chambers J.Q., Eamus D. et al. (2005). Tree allometry and improved estimation of carbon stocks and balance in tropical forests. Oecologia 145, 87–99.

Confalonieri R., Rosenmund A.S., Beruth B. (2009). An improved model to simulate rice yield. Agronomy for Sustainable Development, Springer Verlag/EDP Sciences/INRA, 2009, 29 (3).

Congalton, R.G. and Green, K. 2008 Assessing the Accuracy of Remotely Sensed Data: Principles and Practices, Second Edition (Google eBook).

Ding Y., Zang R., Liu S., He F., Letcher S.G. (2012). Recovery of woody plant diversity in tropical rain forests in southern China after logging and shifting cultivation. Biological Conservation, 145, 225–233.

Englhart S., Jubanski J., Siegert F. (2013). Quantifying Dynamics in Tropical Peat Swamp Forest Biomass with Multi-Temporal LiDAR Datasets. Remote Sens. 5, 2368–2388.

Imai N., Seino T., Aiba S., Takyu M., Titin J., Kitayama, K. (2012). Effects of selective logging on tree species diversity and composition of Bornean tropical rain forests at different spatial scales. Plant Ecology, 213, 1413–1424.

Imai N., Tanaka A., Samejima H., Sugau J.B., Pereira J.T., Titin J. et al. (2014). Tree community composition as an indicator in biodiversity monitoring of REDD+. Forest Ecology and Management, 313, 169–179.

Ioki K., Tsuyuki S., Hirata Y., Phua M.H., Wong W.V.C, Ling Z.Y. et al. (2016). Evaluation of the similarity in tree community composition in a tropical rainforest using airborne LiDAR data. Remote sensing or Environment 173, 304-313.

IPCC (2006). IPCC Guidelines for National Greenhouse Gas Inventories. Prepared by the National Greenhouse Gas Inventories Programme. Eggleston, H.S., Buendia, L., Miwa, k., Ngara, T.and Tanabe, K.(Eds).Published: IGES, Japan.

Jubanski J., Ballhorn U., Kronseder K., Siegert F. (2013). Detection of large above-ground biomass variability in lowland forest ecosystems by airborne LiDAR. Biogeosciences 10, 3917–3930.

Konecny K., Ballhorn U., Navratil P., Jubanski J., Page S.E., Tansey K., Hooijer A., Vernimmen R., Siegert F. (2016). Variable carbon losses from recurrent fires in drained tropical peatlands. Glob Change Biol, 22: 1469–1480.

Magurran A.E., McGill B.J. (2011). Biological diversity: Frontiers in measurement and assessment. New York: Oxford University Press.

Navratil P. (2012). Survey on the Land Cover Situation and Land-Use Change in the Ditricts Kapuas Hulu and Malinau, Indonesia. Final Report for assessment of district and KPH wide REL assessment. Forest and Climate Change Program (FORCLIME).

Richter R., Schläper D. (2014). Atmospheric / Topographic Correction for Satellite Imagery. 1–238.

Su J.C., Debinski D.M., Jakubauskas M.E., Kindscher K. (2004). Beyond species richness: Community similarity as a measure of cross-taxon congruence for coarsefilter conservation. Conservation Biology, 18, 167–173.

Zanne A.E., Lopez-Gonzalez G., Coomes D.A., Ilic J., Jansen S., Lewis S.L., Miller R.B. et al. (2009). Global wood density database. Dryad. Identifier: http://hdl.handle.net/10255/dryad.235.